

Large-Scale Flow Response to the Breaking of Mountain Gravity Waves

François Lott,

LMD, Ecole Normale Supérieure; flott@lmd.ens.fr

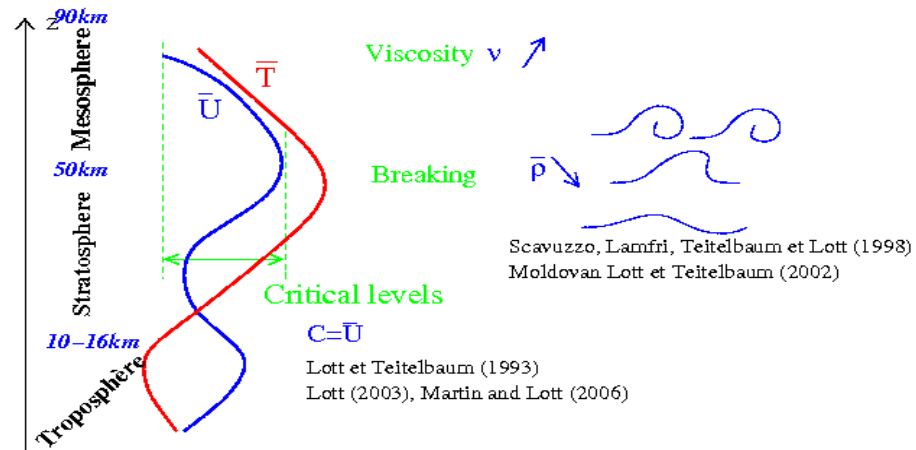
- 1) General: gravity waves and their impact on climate
- 2) Regional and synoptic impacts of mountain gravity waves breaking
 - observations
 - Some diagnostics tools
 - Parameterization in weather prediction and climate models
- 3) Interaction between a front and an idealised mountain massive
 - Balanced response
 - Inertio-gravity waves re-emission (non balanced response)

I General: Gravity Waves and their Impact on Climate

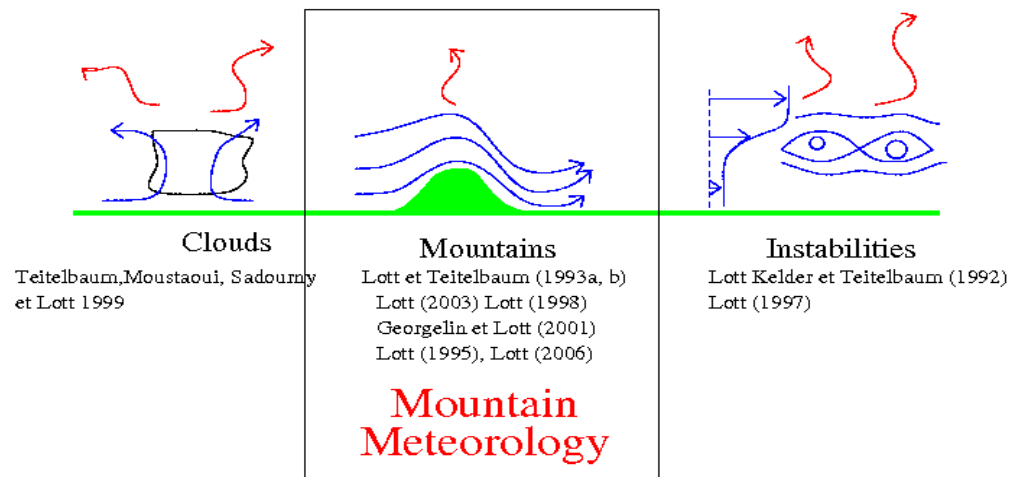
Propagation and interaction with the mean flow

Gravity Wave and Mountain Meteorology (Theory and Observations)

→ Propagation and interaction with the large-scale (mean) flow



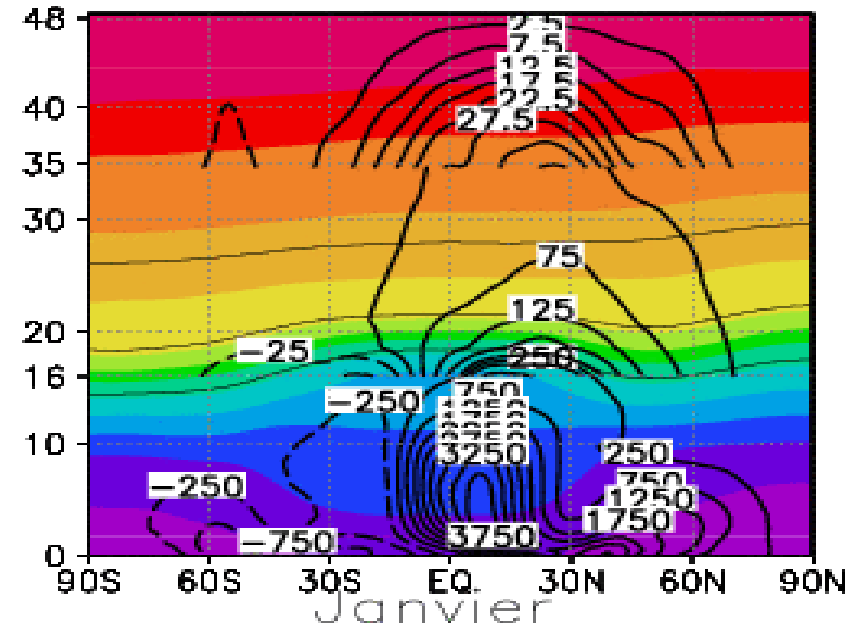
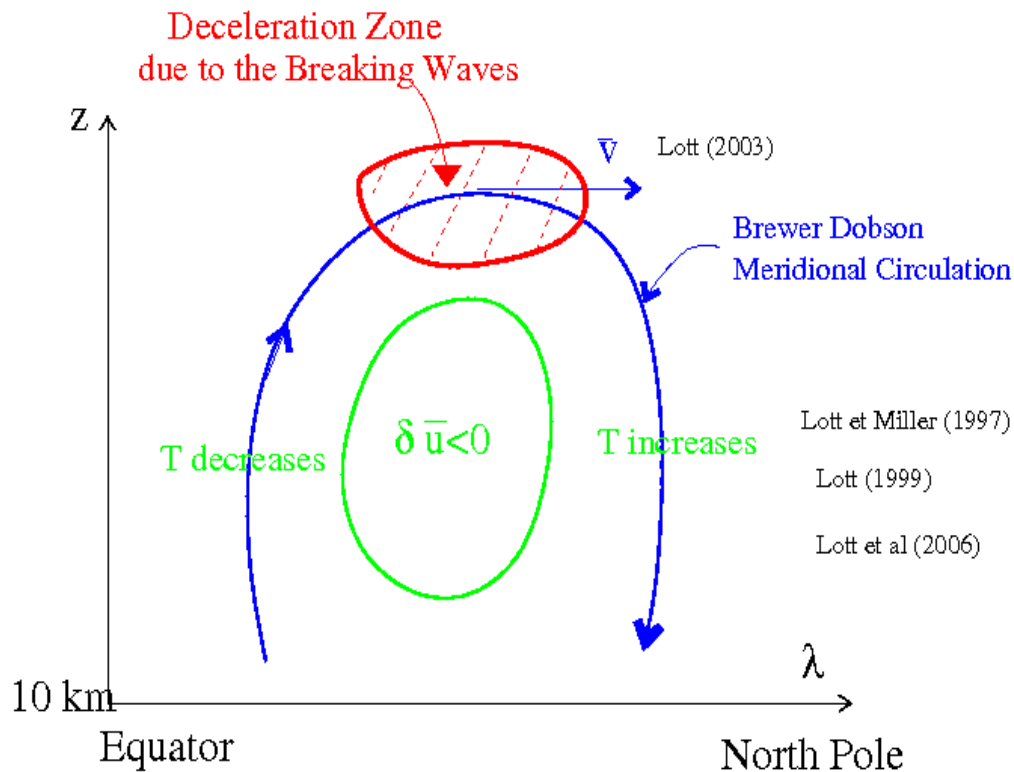
→ Sources:



Sources

I General: Gravity Waves and their Impact on Climate

Impact on the zonal mean flow



Correct systematic errors on T and u

Transports ozone from the tropics toward the high latitudes (crucial in the present context of the development of coupled dynamic-chemistry climate models)

Streamfunction of the Brewer-Dobson circulations (ECMWF data)

In good part due to the breaking of planetary scale waves, but the breaking of gravity waves also make a significant contribution to this circulation

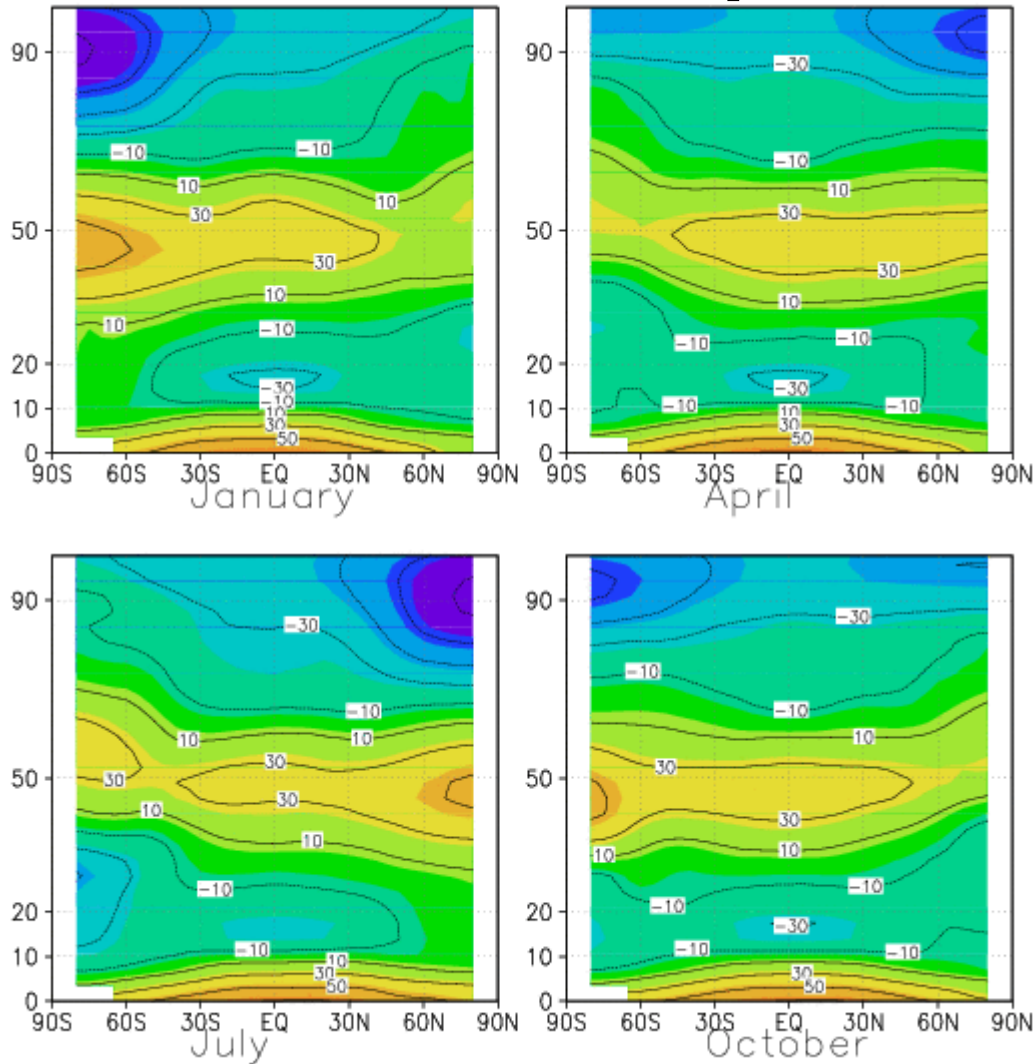
I General: Gravity Waves and their Impact on Climate

Zonal mean for Temperature in the middle atmosphere (CIRA data)

T(K)-230

Solstices

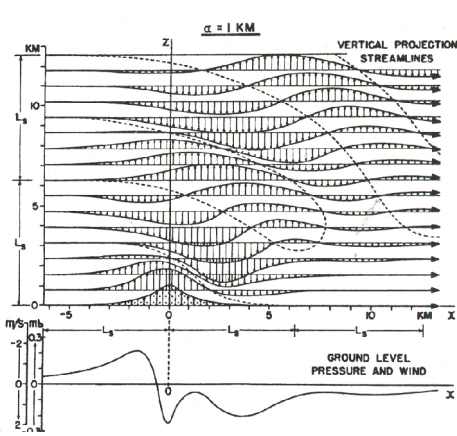
Equinoxes



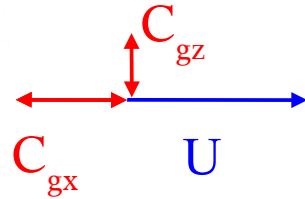
- There is a pronounced minimum in T at the equatorial tropopause during all seasons (Increased IR absorption due to water vapor in the tropics)
- In the stratosphere ($20\text{km} < z < 50\text{km}$), T also decreases from the summer pole to the winter pole.
- At the stratopause (50km) in the summer hemisphere there is a max in T (Maximum insolation of the Ozone layer).
- During Solstices and in the 1/2-top mesosphere (70-90km) T increases from the summer pole to the winter pole!!!
- During solstices and at the summer pole at the mesopause ($z=80\text{—}100\text{km}$) there is an absolute minima in Temperature.

II Regional and Synoptic Impacts of mountain Gravity Waves breaking

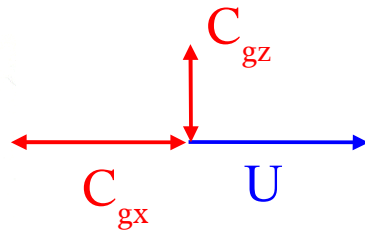
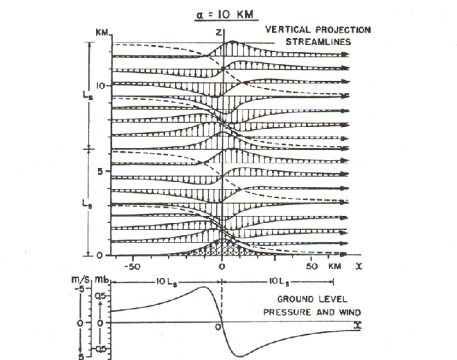
Mountain Waves (linear 2D theory from Queney (1948))



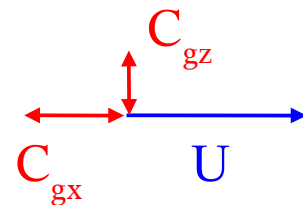
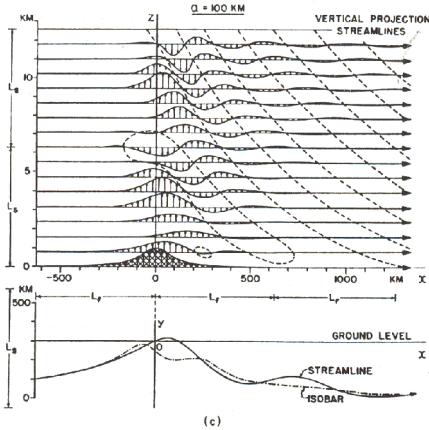
$$U=10\text{m/s}, N=0.01\text{s}^{-1}, f=0.0001\text{s}^{-1}$$



$d=1\text{km}, U/d \sim N$, non-hydrostatic effects



$d=10\text{km}$, Hydrostatic non-rotating



$d=100\text{km}, U/d \sim f$
Hydrostatic-Rotating
Régime

Fig. 8.9. (continued)

For linear stationary waves, the momentum flux due to the waves equal the surface pressure drag:

$$\int_{-\infty}^{\infty} \int_{-\infty}^{\infty} \rho \vec{u}' w' dx dy(z) = -\mathcal{D}$$

The surface pressure drag is:

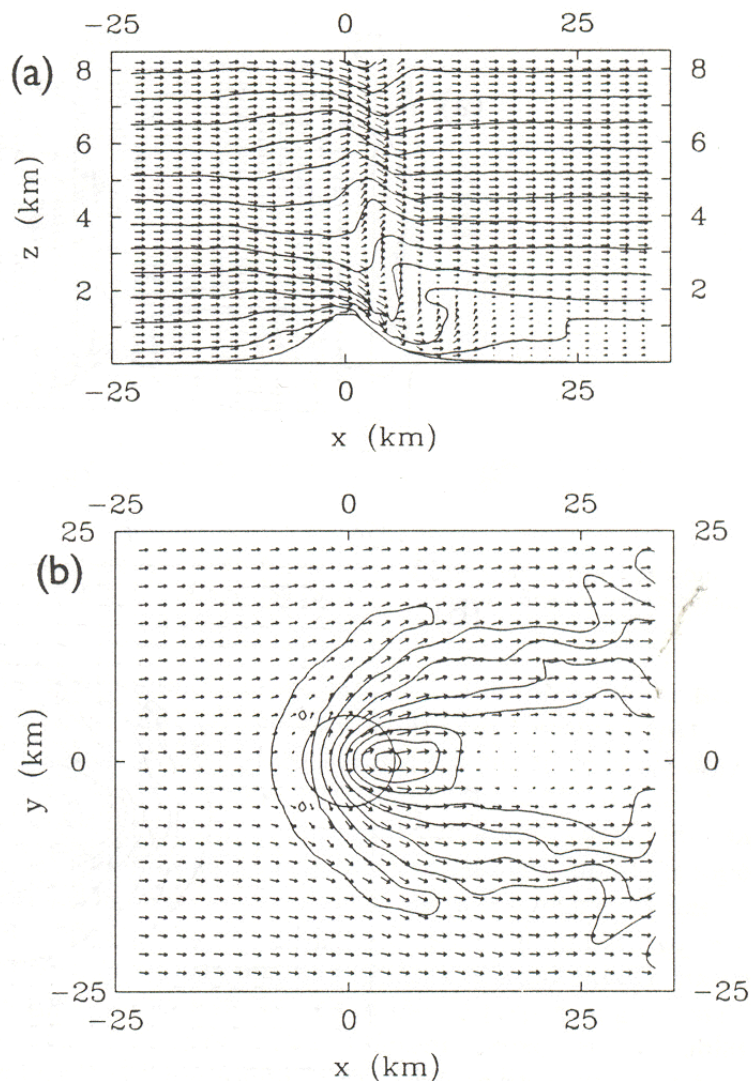
$$\mathcal{D} = \int_{-\infty}^{\infty} \int_{-\infty}^{\infty} p' \vec{\nabla} h dx dy$$

(it is a little more complicated when $f \neq 0$)

II Regional and Synoptic Impacts of mountain Gravity Waves breaking Mountain Waves (non-linear 3D effects from Miranda and James (1992))

$$U=10\text{m/s}, N=0.01\text{s}^{-1}, h_{\text{max}} \sim 1\text{km}$$

Note:



The fact that the isentropic surfaces are almost vertical downstream and at low level: this indicates wave breaking

The strong “Foehn” downstream

The residual gravity waves propagating aloft

The apparent deceleration of the low-level winds far downstream of the obstacle.

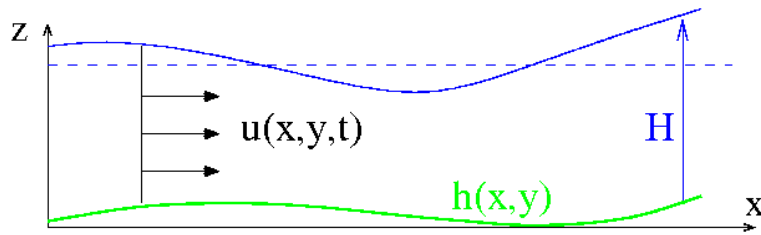
Question:

How can we quantify the reversible motion (due to the presence of the wave) from the irreversible effects that due to its breaking?

II Regional and Synoptic Impacts of mountain Gravity Waves breaking

The example of the Hydraulic Jumps in the Shallow water Equations

Schar et Smith 1992



Shallow water Equations, with dissipative effects represented by X, Y :

$$\frac{Du}{Dt} - fv = -g \frac{\partial h + H}{\partial x} + X$$

$$\frac{Dv}{Dt} + fv = -g \frac{\partial h + H}{\partial y} + Y$$

$$\frac{DH}{Dt} + H \left(\frac{\partial u}{\partial x} + \frac{\partial v}{\partial y} \right) = 0$$

Equation for the absolute vorticity: $\xi_a = \partial_x v - \partial_y u + f$:

$$\frac{\partial \xi_a}{\partial t} + \vec{\nabla} \cdot (\vec{u} \xi_a + \vec{J}_N) = 0$$

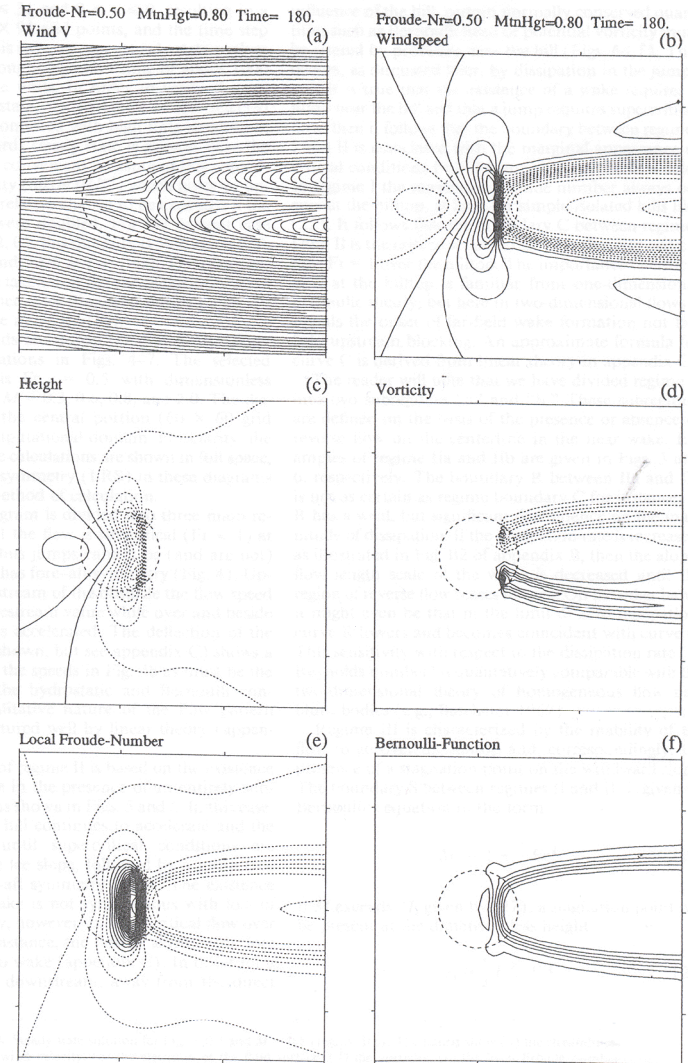
Advective flux of absolute vorticity: $\vec{u} \xi_a$

Non-advective flux of absolute vorticity:

$$\vec{J}_N = -Y \vec{e}_x + X \vec{e}_y$$

Without dissipation, $X = Y = 0$, $\vec{J}_N = 0$ the potential vorticity $Q = \xi_a / H$ is conserved:

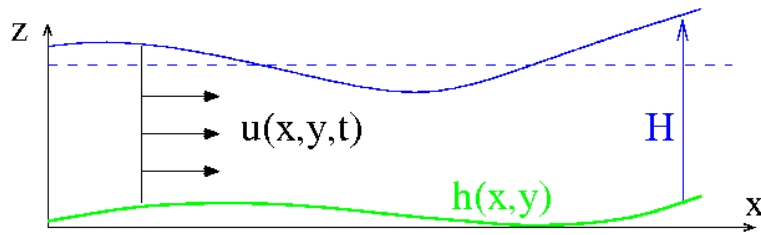
$$\frac{DQ}{Dt} = 0$$



II Regional and Synoptic Impacts of mountain Gravity Waves breaking

The example of the Hydraulic Jumps in the Shallow water Equations

Schar et Smith 1992



The St Venant equations can also be written:

$$\frac{\partial \vec{u}}{\partial t} + \vec{k} \times (\xi_a \vec{u} + \vec{J}_N) + \vec{\nabla} B = 0$$

where B is the Bernoulli Head (ask your plumber about it):

$$B = \frac{u^2 + v^2}{2} + g(h + H)$$

Its evolution is given by:

$$\frac{DB}{Dt} = +g \frac{\partial H}{\partial t} + Xu + Yv$$

(the lost of Head is related to the dissipative forces working against the flow):

Important:

In the stationary case, the Bernoulli function B is the streamfunction of the total flux of absolute vorticity:

$$\xi_a \vec{u} + \vec{J}_N = \vec{k} \times \vec{\nabla} B$$

The potential vorticity and the Bernoulli function show where the mountain wave breaks (a steady non-dissipative wave produces no anomaly of Q and B)

These properties apply to all “dynamically consistent” systems of equations

The effect of the mountain is to produce a force X, Y in the flow at the place where the surface wave drag is restituted (e.g. The breaking zone)

A very comparable behaviour occurs when the fluid surface intersects the obstacle

II Regional and Synoptic Impacts of mountain Gravity Waves breaking

The example of the Hydraulic Jumps in the Shallow water Equations

Schar et Smith 1992

Case where the obstacle pierces the surface

Heuristic Description ($f=0$)

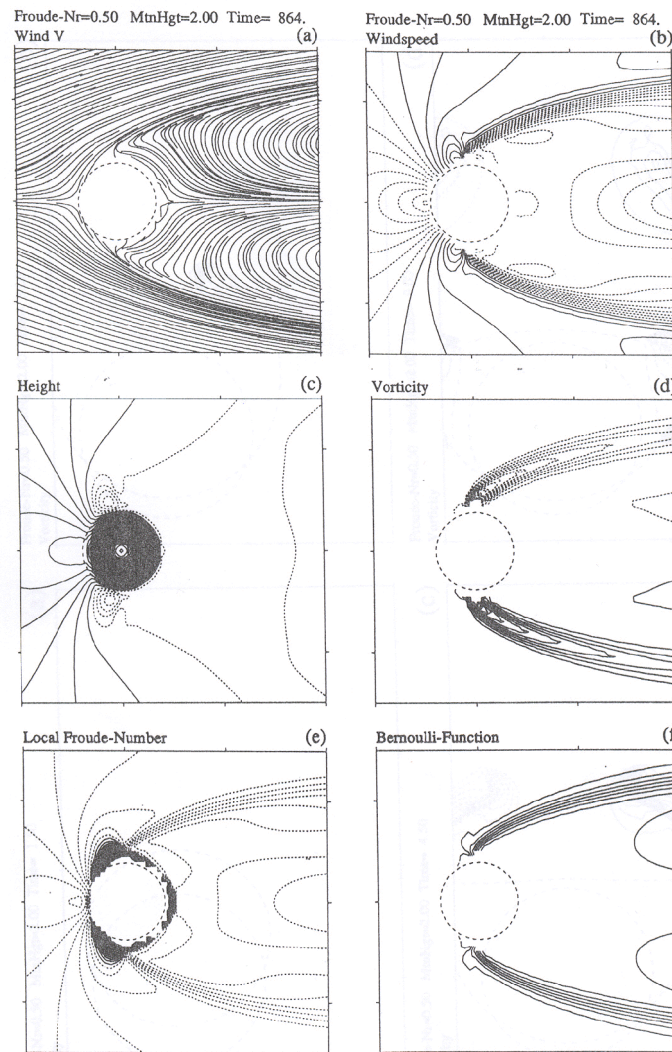
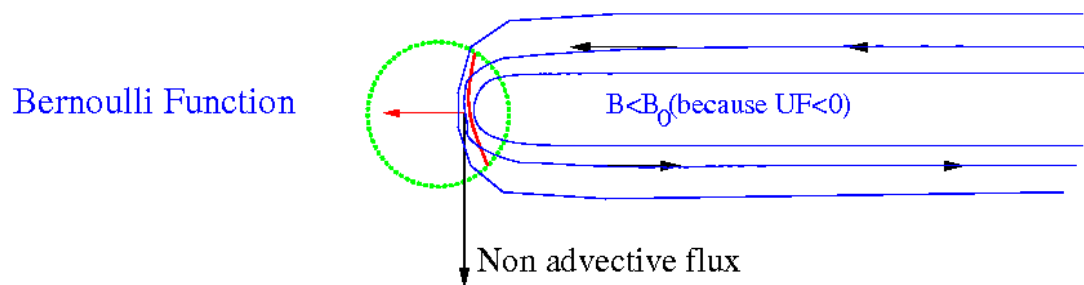
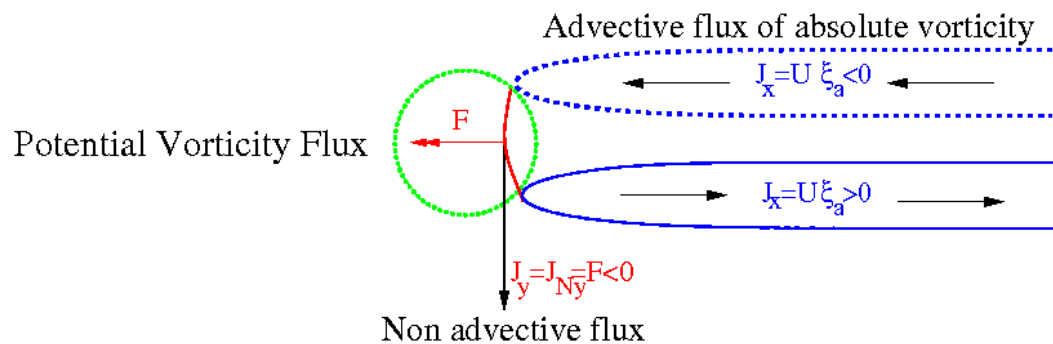
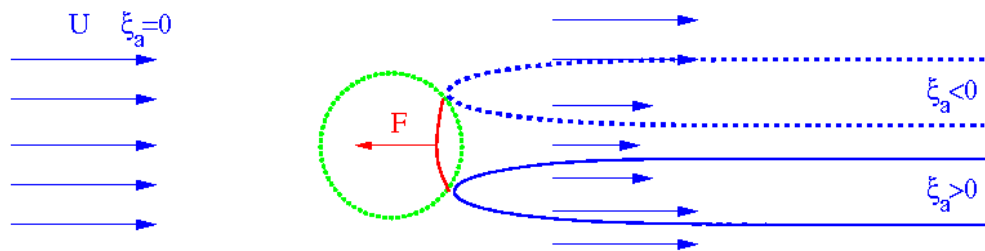
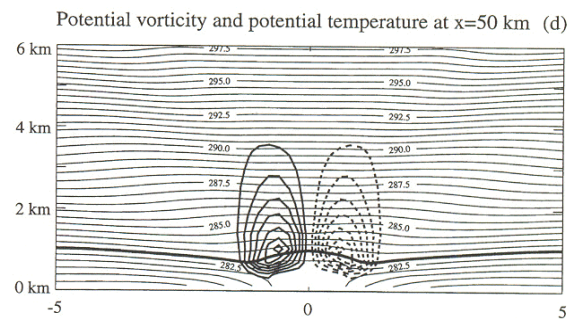
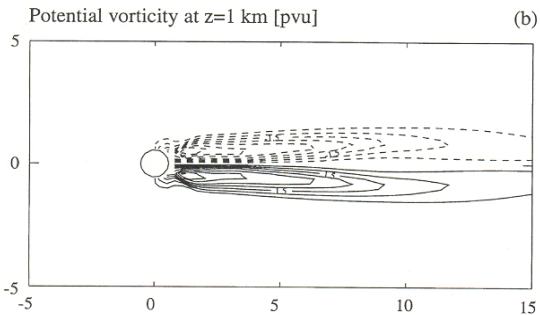
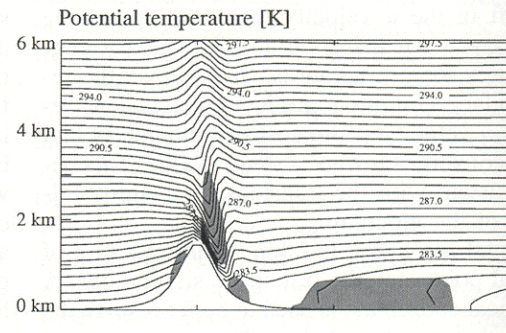
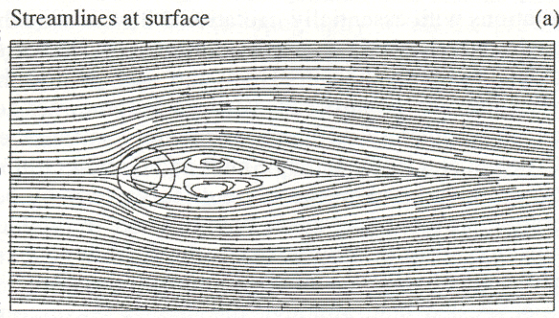


FIG. 7. As in Fig. 6 but for $Fr_\infty = 0.5$ and $M = 2$ (regime III). Here the mountain pierces the fluid surface (blank areas). Panel (c) shows the topography in pierced regions of the flow.

II Regional and Synoptic Impacts of mountain Gravity Waves breaking Extension to a continuously stratified fluid

Schar et Durran 1997



You can see isentropic surfaces as the free surface of the shallow water equations (the PV flux is then // to the isentropes)

The place where the wave break is then the equivalent of the hydrolic jump

II Regional and Synoptic Impacts of mountain Gravity Waves breaking

Observations

Lott (1995) et Georgelin and Lott (2001)
For the PYREX dataset, Bougeault et al. (1990)

Le central transect
during PYREX

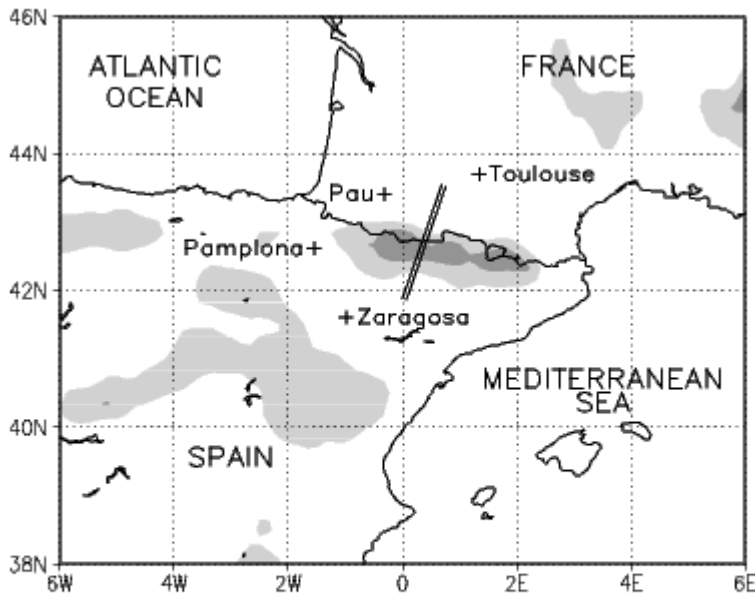
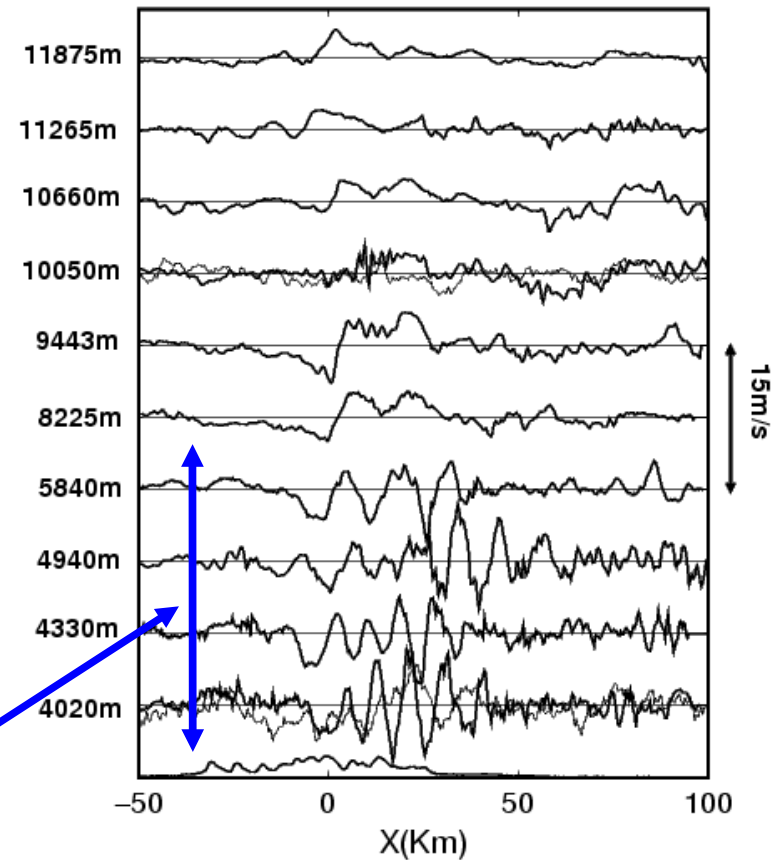


Figure 1: Smoothed terrain elevation and PYREX data used. + denotes the location of the high resolution soundings. The two thick lines indicate the airplane paths during the IOP 3. The light and dark shaded areas denote terrain elevation above 1000m and 1500m respectively.

Mountain waves seen by 10 aircraft
flights above the transect



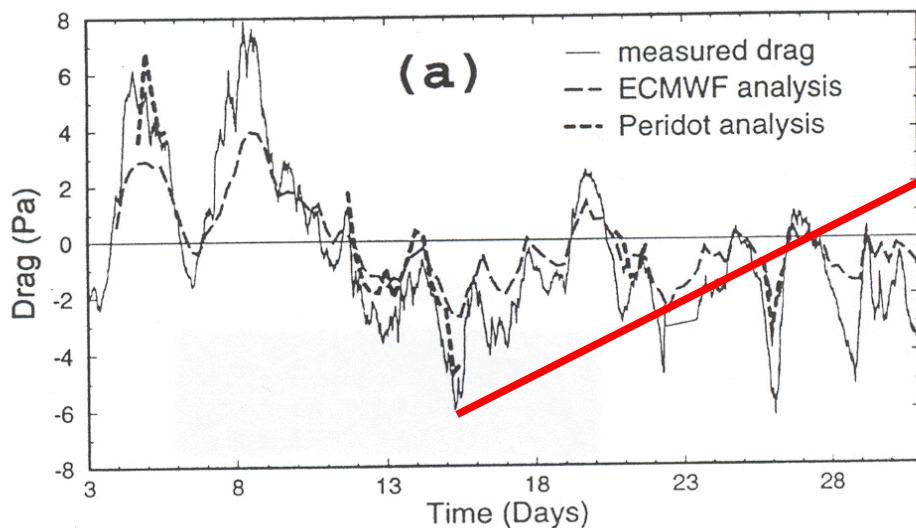
Ondes piégées
(Georgelin et Lott 2001)

Figure 2: Observed vertical velocities from different Aircraft legs. 15 October 1990 around 6 UTC. Thick lower curve represent the Pyrénées, the thin curve at the Z=4km and Z=10km are red noises surrogate with characteristics adapted to the measured vertical velocity at that levels.

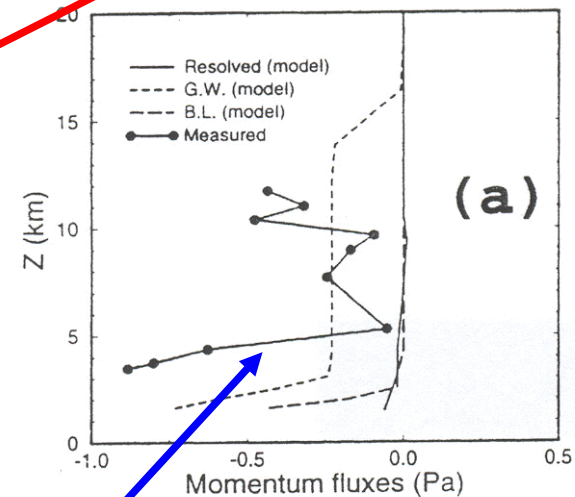
II Regional and Synoptic Impacts of mountain Gravity Waves breaking Observations

Lott (1995) et Georgelin and Lott (2001)
For the PYREX dataset, Bougeault et al. (1990)

The surface pressure drag measured by micro barographs located along the transect (October 1990)



The momentum flux measured by the aircrafts aloft the transect, the 15 October 1990



Effect of the trapped lee waves
(Georgelin et Lott 2001)

Note that the momentum flux aloft is one order of magnitude smaller than the surface drag. This indicates low level wave breaking, and that the flow passes around the hill, detaches on its flank, forming a wake downstream of the mountain.

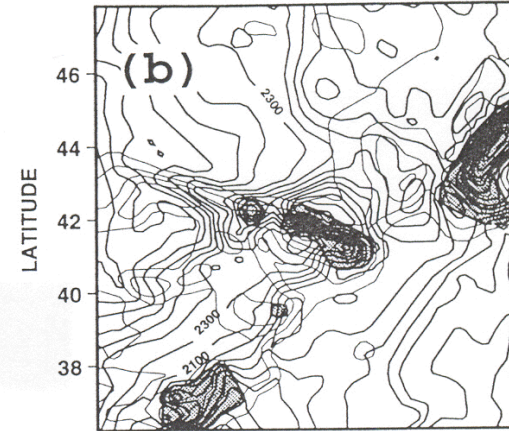
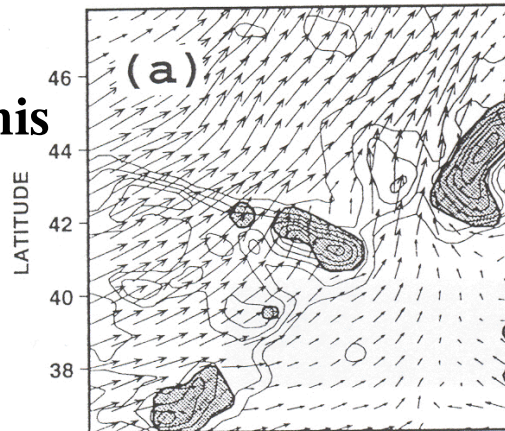
II Regional and Synoptic Impacts of mountain Gravity Waves breaking

Observations (?): isentropic diagnostics of the associated mesos-scale reanalysis (15 October 1990)

Lott (1995)

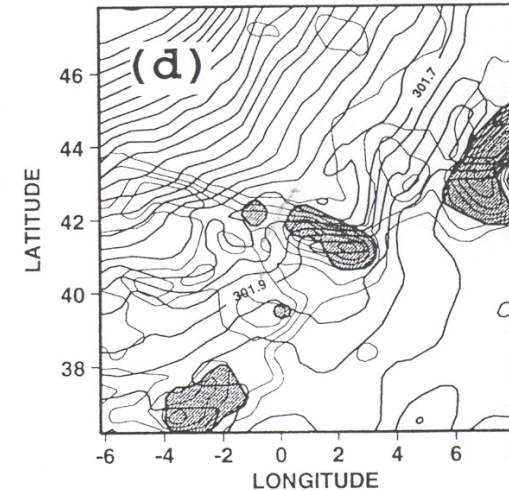
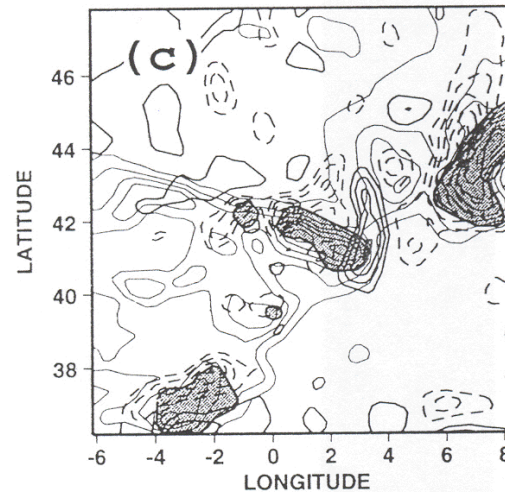
$\theta=302\text{K}$, the shaded areas are where the mountains intersect this isentrope

Wind



Altitude

Absolute Vorticity



Bernoulli Head

Figure 9. Peridot analysis, 12 UTC 15 October 1990. Orography (contour interval = 400 m) and flow diagnostics on the isentropic surface $\theta = 302$ K. In the shaded area, the isentrope goes below the lowest model level. (a) wind; (b) elevation, contour interval = 200 m; (c) isentropic relative vorticity, contour interval = $0.5 \times 10^{-4} \text{s}^{-1}$, negative values dashed and (d) Bernoulli function, contour interval = 100J kg^{-1} .

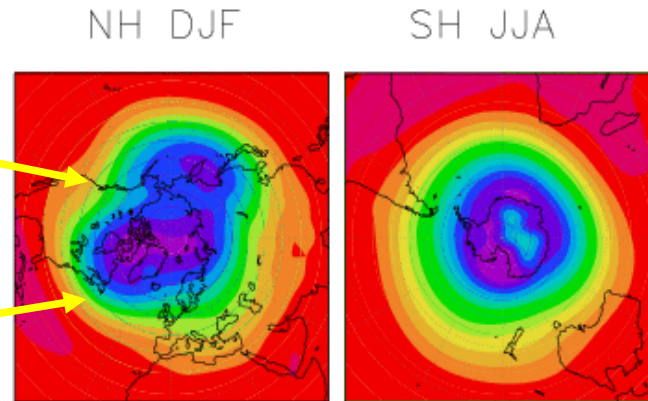
II Regional and Synoptic Impacts of mountain Gravity Waves breaking

Significance of mountains at the planetary scales

Lott (1999)

Ridge (vorticity $\xi < 0$)

Trough (vorticity $\xi > 0$)



NCEP Reanalysis, geopotential height at 700hPa (winter)

Potential vorticity conservation (Quasi-Geostrophic approximation):

$$\frac{d(\xi + f)\theta_z}{dt} = 0.$$

Relative vorticity:

$$\xi = \partial_x v_g - \partial_y u_g$$

The isentropic surfaces are almost like material surfaces (In the adiabatic frictionless context):

$$\frac{d\theta}{dt} = 0.$$

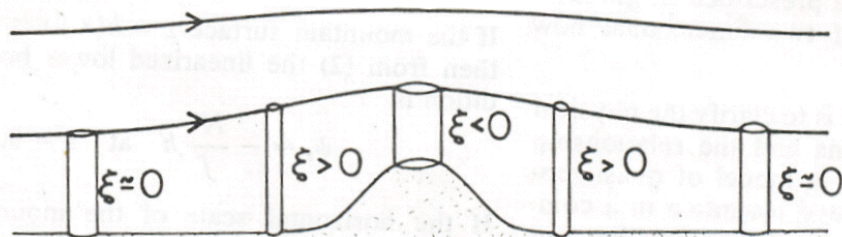


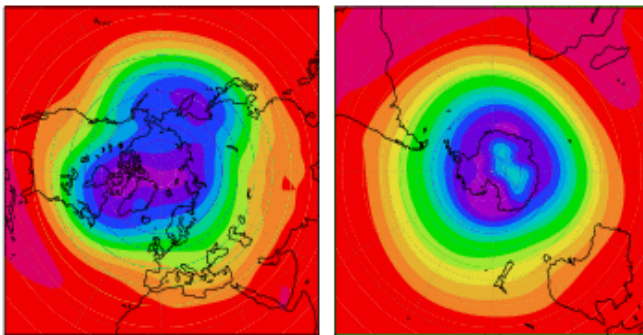
FIG. 1. The quasi-geostrophic stratified flow over a mountain. The vertical displacement of potential temperature surfaces becomes weaker but more widespread aloft. The stretching of vortex line near the ground causes strong anticyclonic vorticity over the mountain and weaker cyclonic vorticity surrounding the mountain. Further aloft, the vorticity distribution broadens and becomes weaker. (After Buzzi and Tibaldi.)

II Regional and Synoptic Impacts of mountain Gravity Waves breaking Parameterization in General Circulation Models Lott and Miller (1997), Lott (1999), Lott et al. (2005)

Significance of mountains at the planetary scales

NH DJF

SH JJA

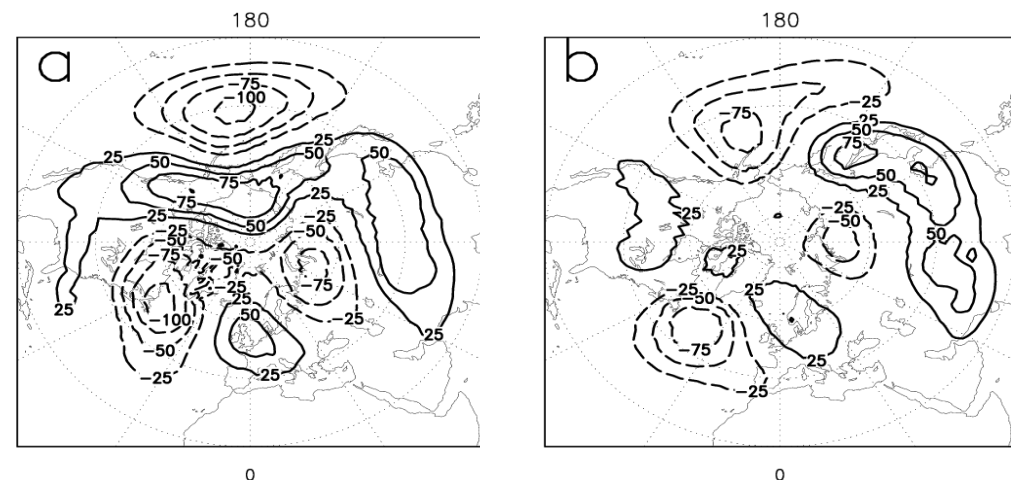


NCEP Reanalysis, geopotential
height at 700hPa (winter)

Parameterization and impacts

Without

With

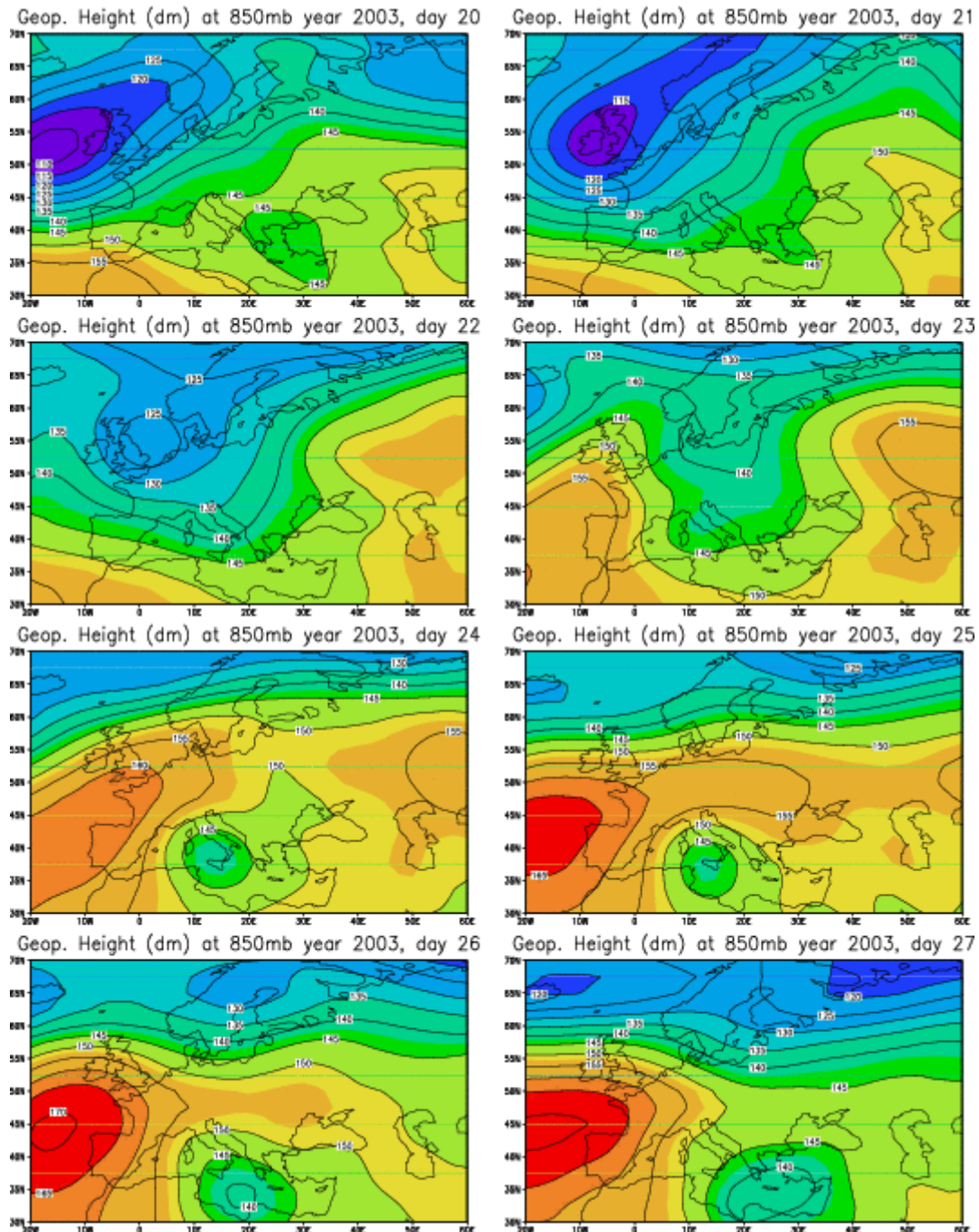


Error maps of Z at 700hPa, NCEP-LMDz (winter)

- Physical principles underneath the parameterization: include gravity waves, low level wave breaking, trapped lee waves, low-level blocking and the associated Downstream wakes.
- Opérationnel at ECMWF, LMD, MPI, the low level blocking inspires other centres

III Interaction between a front and an idealised mountain massive

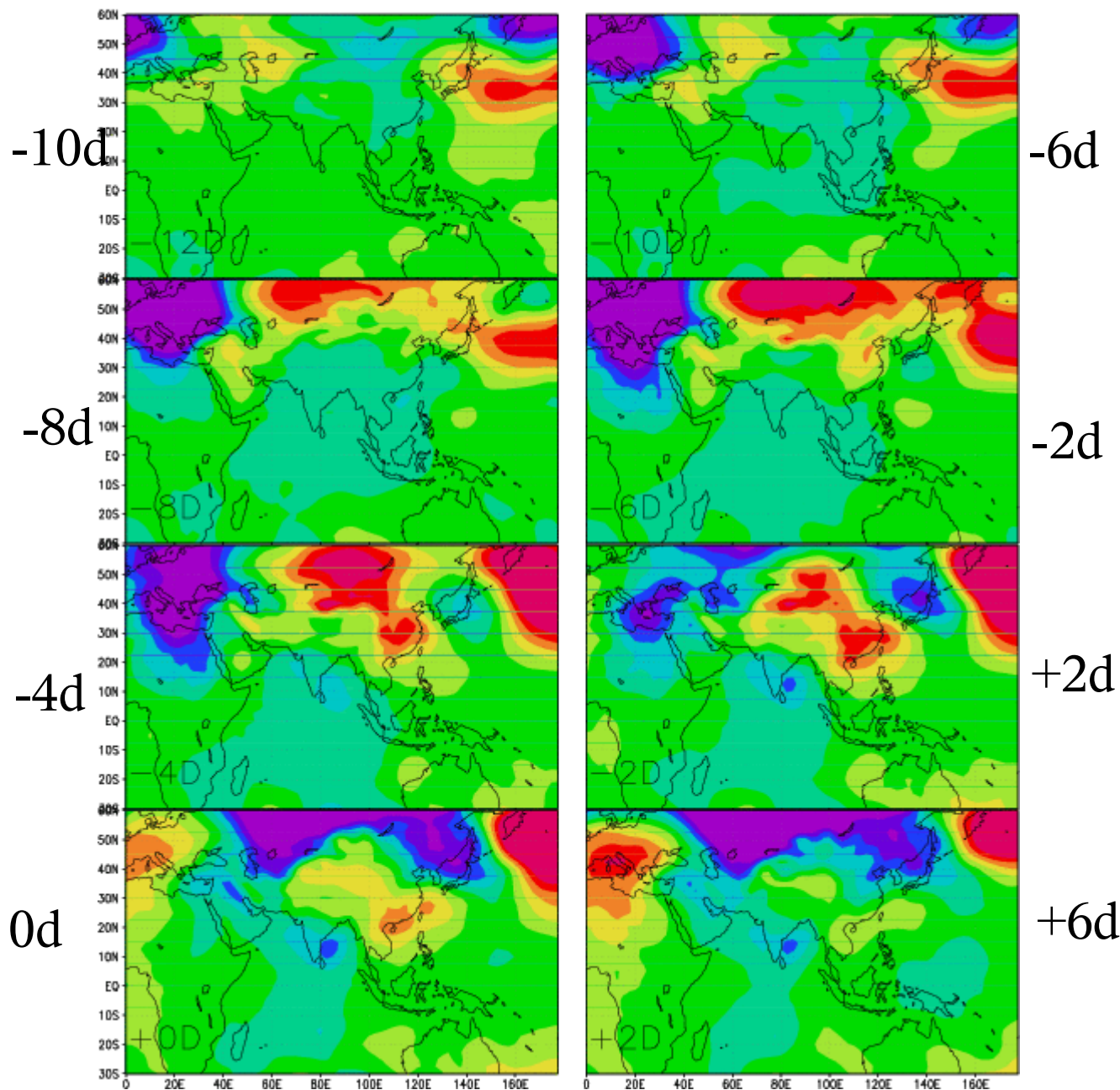
A case of lee cyclogenesis (NCEP data, 850hPa height)



III Interaction between a front and an idealised mountain massive

Variability over the Bay of Bengal (NCEP data, Surface pressure)

ISL SLP COMPOSITE (70-03)
Key: PWAT over Bay of B



Composite of surface pressure keyed to the Precipitation over the bay of Bengal

Note again the anomaly descending along the Eastern flank of the massive.

These effects are probably more barotropic than the Eady Wave dynamics to be discussed in the rest of the talk

III Interaction between a front and an idealised mountain massive

A theory for mountain lee cyclogenesis (Smith 1979)

Mountain profile:

$$\mathcal{H}(\mathbf{x}) = H_0 e^{-\frac{x^2+y^2}{2L^2}}$$

Background wind and Potential Temperature profiles:

$$\mathbf{U}(z) = U(z) \mathbf{e}_x + V_0 \mathbf{e}_y = \Lambda z \mathbf{e}_x + V_0 \mathbf{e}_y,$$

$$\Theta_b(y, z, t) = \theta_r + \theta_{0z} z + \Theta_y y$$

Brunt Vaisala frequency, thermal wind balance, and Richardson number:

$$N^2 = \frac{g \theta_{0z}}{\theta_r}, \quad \Theta_y = -\frac{\Lambda f \theta_r}{g}, \quad Ri = \frac{N^2}{\Lambda^2}$$

Semi-Geostrophic linearised equations (inside the flow):

$$(\partial_t + \mathbf{U} \nabla) u_g + w \Lambda - f v + \partial_x \phi = 0$$

$$(\partial_t + \mathbf{U} \nabla) v_g + f u + \partial_y \phi = 0$$

$$(\partial_t + \mathbf{U} \nabla) \theta + v \Theta_y + w \theta_{0z} = 0;$$

$$\partial_x u + \partial_y v + \partial_z w = 0.$$

Geostrophic wind and hydrostatic relationship:

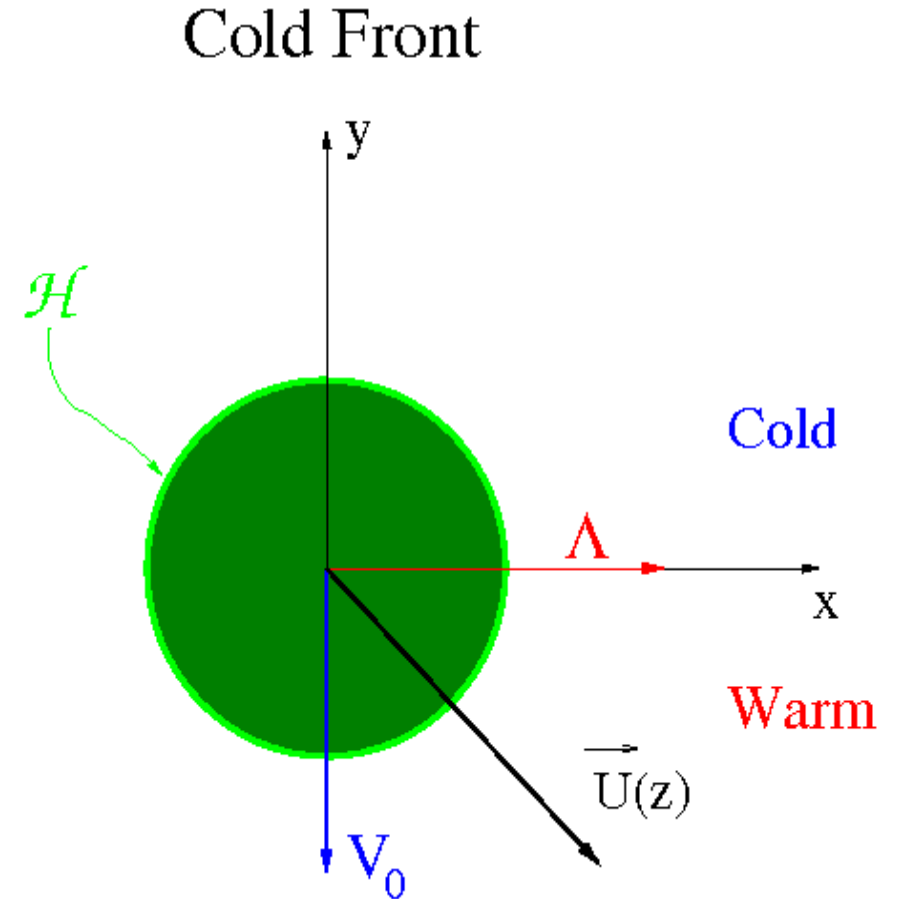
$$u_g = -\partial_y \phi / f \quad v_g = \partial_x \phi / f \quad g \theta / \theta_r = \partial_z \phi.$$

In this system the Semi-Geostrophic potential vorticity is conserved. For the disturbance PV this yields:

$$q(\mathbf{x}, z, t) = \theta_{0z} \left((1 - Ri^{-1}) \partial_x v_g - \partial_y u_g \right) + \Lambda \partial_y \theta + \Theta_y \partial_z u_g + f \partial_z \theta = 0$$

Boundary condition at $z = 0$ (no tropopause):

$$(\partial_t + \mathbf{U}(0) \cdot \nabla) \theta + v \Theta_y = -\theta_{0z} \mathbf{U}(0) \cdot \nabla \mathcal{H} \quad \text{in } z = 0$$



III Interaction between a front and an idealised mountain massive

A theory for mountain lee cyclogenesis (Smith 1979)

The free boundary Eady Waves

Resolution in the spectral space:

$$\phi(\mathbf{x}) = \int_{-\infty}^{\infty} \int_{-\infty}^{\infty} \hat{\phi}(\mathbf{k}) e^{-i\mathbf{k}\cdot\mathbf{x}} d\mathbf{k} dl$$

A solution with zero PV inside the flow:

$$\hat{\phi}(\mathbf{k}, z, t) = \hat{\phi}_u(\mathbf{k}, t) e^{-\lambda z}$$

where:

$$\lambda = \lambda_r - i\lambda_i, \quad \lambda_r = \frac{N}{f} \sqrt{1 - Ri^{-1} |\mathbf{k}|}, \quad \lambda_i = l \frac{\Lambda}{f}$$

In this case, the boundary condition becomes:

$$\lambda_r (\partial_t - i\mathbf{k} \cdot \mathbf{U}(\mathbf{0})) \hat{\phi}_u - ik\Lambda \hat{\phi}_u = -i\mathbf{k} \cdot \mathbf{U}(\mathbf{0}) N^2 (1 - Ri^{-1}) \hat{\mathcal{H}}(\mathbf{k})$$

↑
Evolution and advection
of the Temperature
(and pressure) perturbation

↙
Meridional advection
of the Background T
by the perturbation

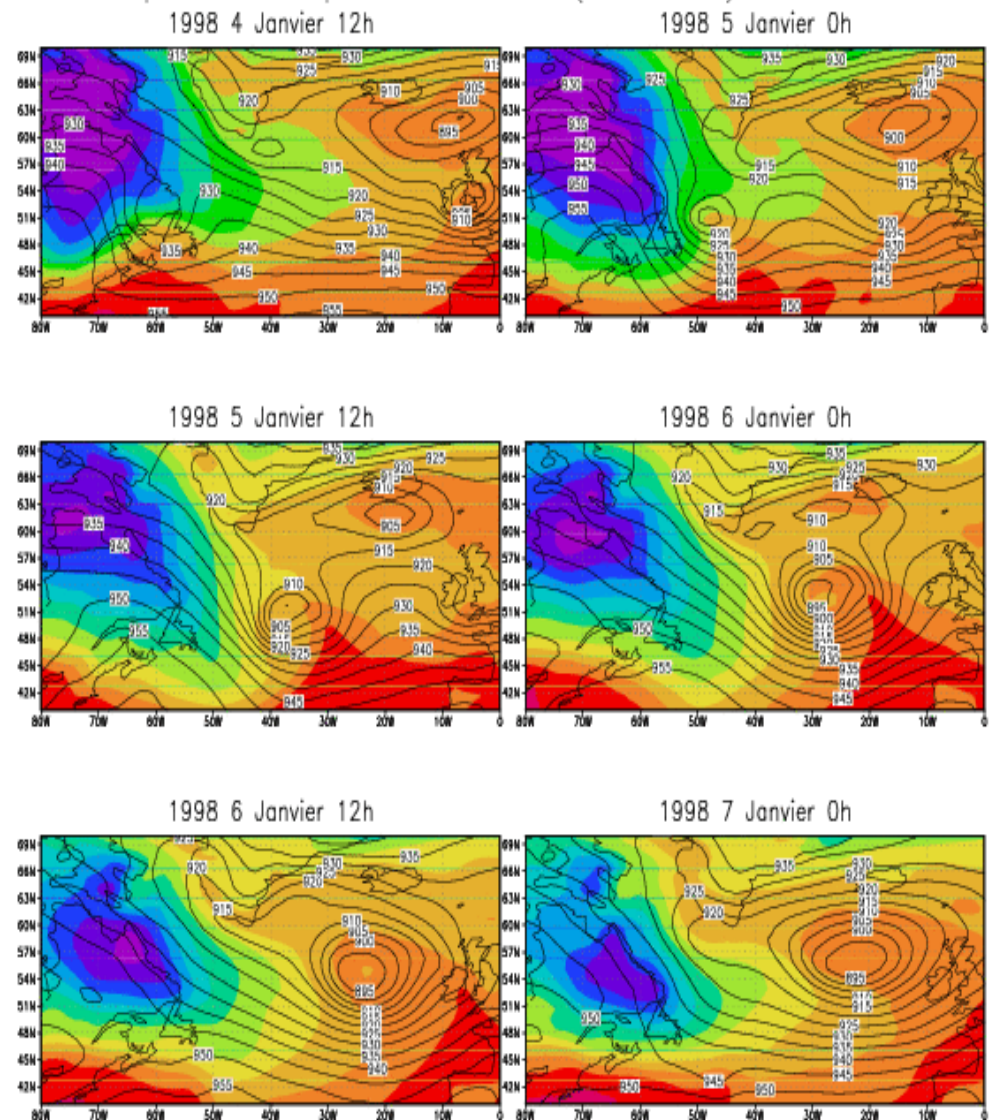
Free Eady waves:

$$\partial_t = i\omega \quad \text{and} \quad \hat{\mathcal{H}} = 0$$

Dispersion relationships:

$$\omega = \mathbf{k} \cdot \mathbf{U}(\mathbf{0}) + k \frac{\Lambda}{\lambda_r}$$

Surface pressure at z=600m (black) and
Surface T (color) during an intense cyclogenesis



III Interaction between a front and an idealised mountain massive

A theory for mountain lee cyclogenesis (Smith 1979)

Forced boundary Eady Waves

Case for which $\phi = 0$ at $t = 0$ and $\mathcal{H} \neq 0$,
numerical resolution of the surface T equation
in the Spectral Space:

$$\lambda_r (\partial_t - i\mathbf{k} \cdot \mathbf{U}(\mathbf{0})) \hat{\phi}_u - ik\Lambda \hat{\phi}_u = -i\mathbf{k} \cdot \mathbf{U}(\mathbf{0}) N^2 (1 - Ri^{-1}) \hat{\mathcal{H}}(\mathbf{k})$$

and back in the physical space.

Parameters:

$$f = 10^{-4} \text{s}^{-1}, N = 10^{-2} \text{s}^{-1}, \Gamma = 410^{-3} \text{s}^{-1},$$

$$H_0 = 800 \text{m}, L = 200 \text{km}$$

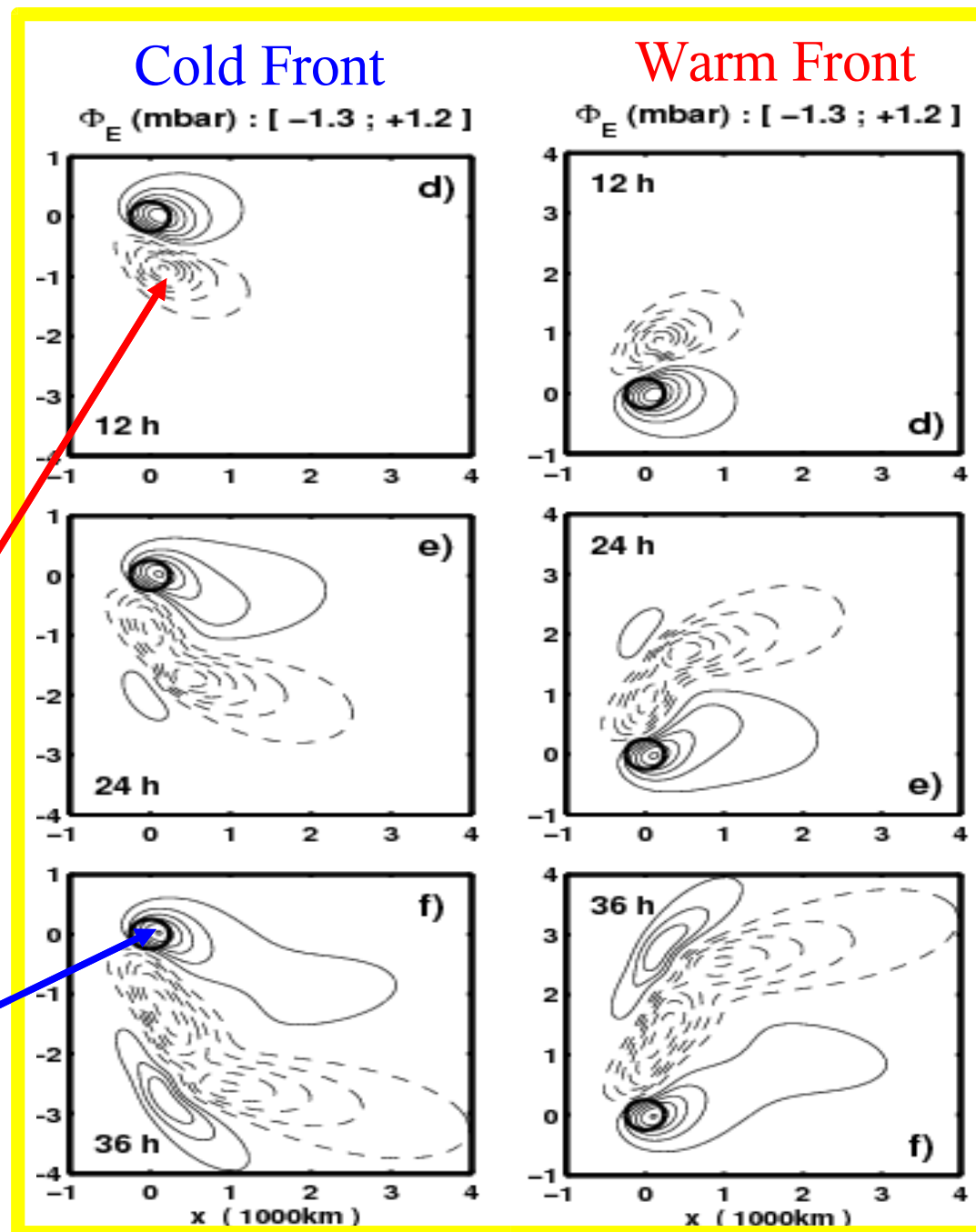
Cold front: $V_0 = -20 \text{m/s}$

Warm front: $V_0 = 20 \text{m/s}$

The cyclogenetic effect is indicated by the
trough developing immediately downstream

It occurs for cold and warm fronts

Over the mountain, the circulation is anti-
cyclonic (ridge)



III Interaction between a front and an idealised mountain massive

Influence of gravity waves on mountain lee cyclogenesis (Martin and Lott 2006)

Mountain profile:

$$h'(\mathbf{x}) = H_0 e^{-\frac{x^2+y^2}{2L^2}} \cos(\mathbf{k}_w \mathbf{x})$$

with $\|\mathbf{k}_w\|L \gg 1$, and $\frac{\|\mathbf{k}_w\| \|\mathbf{U}\|}{f} \gg 1$
 (h' forces gravity waves).

Inflow Semi-Geostrophic Equations:

$$(\partial_t + \mathbf{U}\nabla) u_g + w\Lambda - fv + \partial_x \phi = \mathcal{F}/\rho_r ;$$

$$(\partial_t + \mathbf{U}\nabla) v_g + fu + \partial_y \phi = \mathcal{G}/\rho_r ;$$

$$(\partial_t + \mathbf{U}\nabla) \theta + v\Theta_y + w\theta_{0z} = 0 ;$$

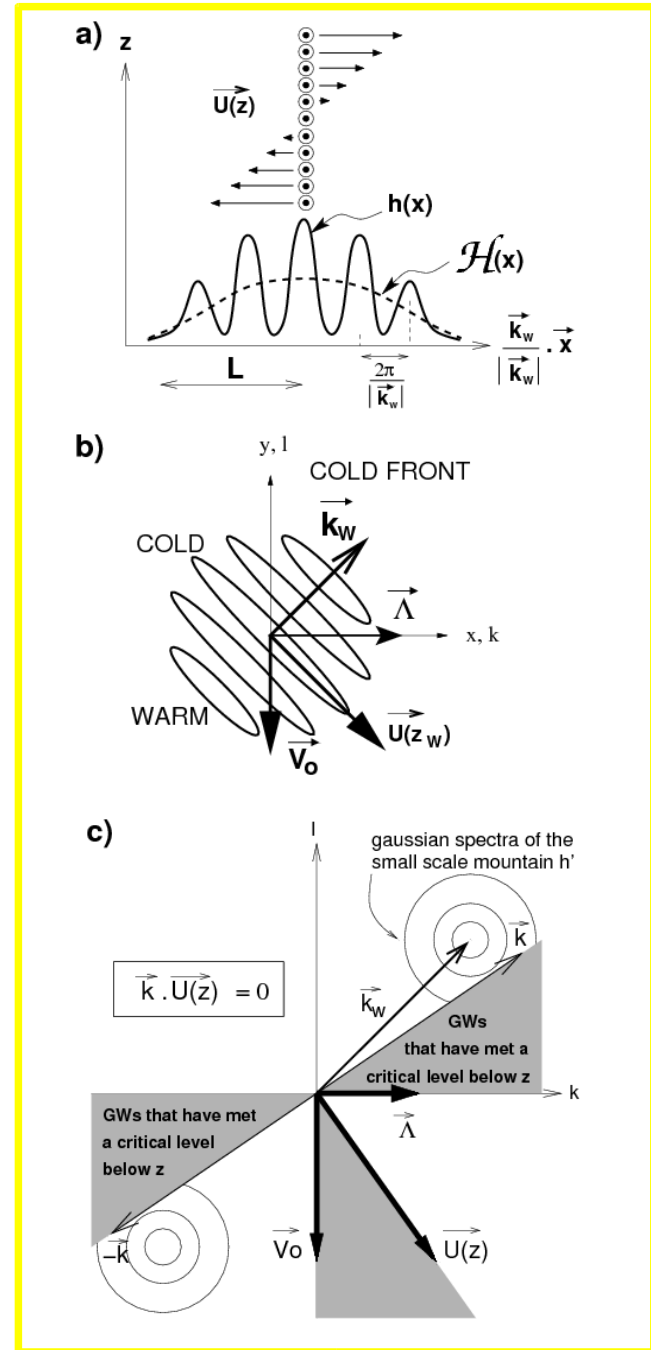
$$\partial_x u + \partial_y v + \partial_z w = 0.$$

\mathcal{F} and \mathcal{G} are the momentum deposition induced by the breaking gravity waves. Here when they reach a Critical Level:

$$\mathbf{k} \cdot \mathbf{U}(z) = 0$$

z_w is the middle of the wave breaking zone:

$$\mathbf{k}_w \cdot \mathbf{U}(z_w) = 0$$



III Interaction between a front and an idealised mountain massive

Evaluation of the Gravity Waves force (Martin and Lott 2006)

The force is distributed horizontally aloft the mountain:

$$\mathcal{F}(\mathbf{x}, z) = \overline{\mathcal{F}}(z) e^{-\frac{x^2+y^2}{L^2}}$$

where the "net" force:

$$\overline{\mathcal{F}}(z) = -\rho_r \frac{d}{dz} \overline{\mathbf{u}' w'}$$

is the divergence of the momentum flux:

$$\overline{\mathbf{u}' w'} = \frac{1}{\pi L^2} \int_{-\infty}^{+\infty} \int_{-\infty}^{+\infty} \mathbf{u}' w' dx dy = \frac{4\pi^2}{\pi L^2} \int_{k=0}^{+\infty} \int_{l=-\infty}^{+\infty} (\hat{\mathbf{u}} \hat{w}^* + \hat{\mathbf{u}}^* \hat{w}) dl dk$$

Following the linear stationary theory for mountain waves in the presence of a critical level in z_c (Shutts 1995, 1998):

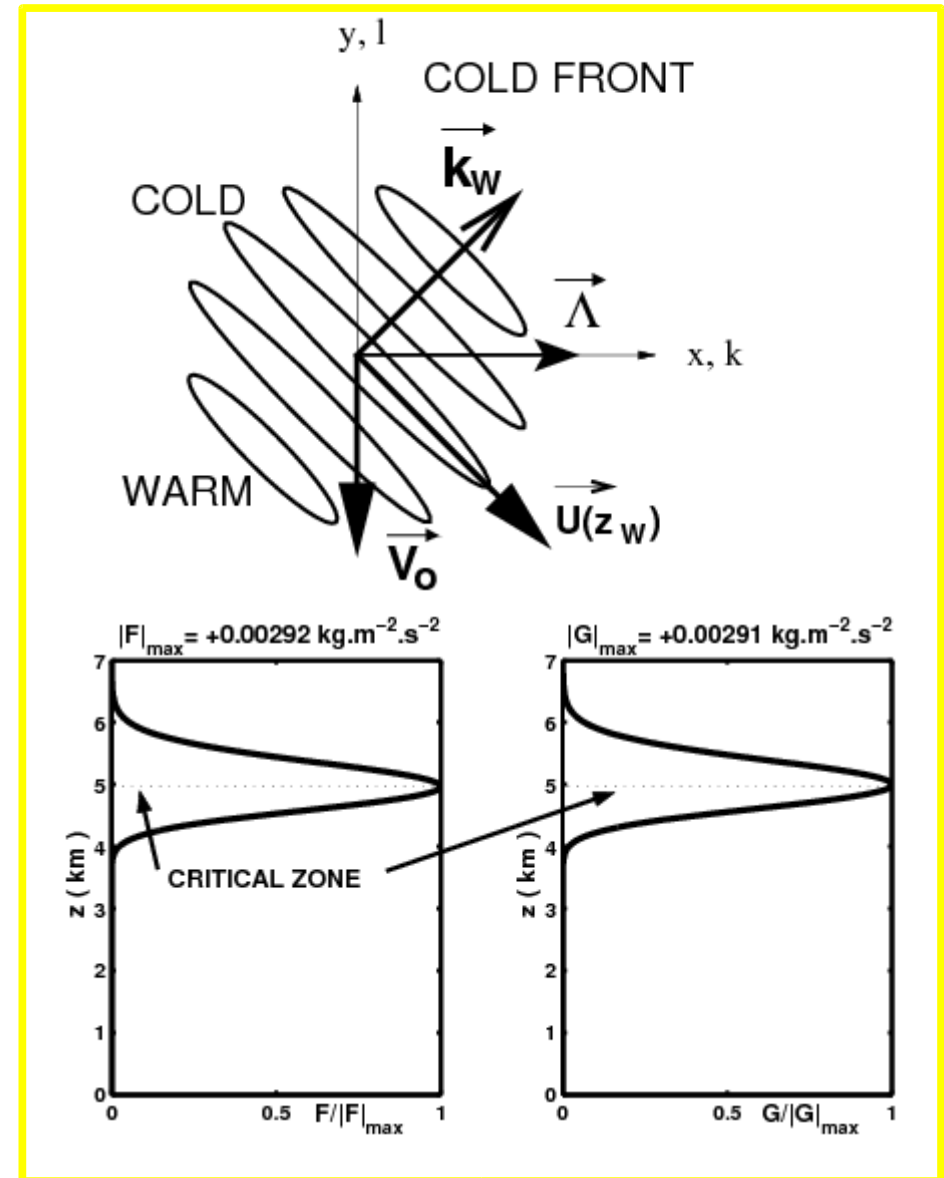
$$\hat{w}'(z) = -i\mathbf{k}U_0 \hat{h}' (1 - z/z_c)^{1/2 + i\epsilon} \quad , \quad \text{for } z < z_c$$

$$\hat{w}'(z) \approx 0 \quad \text{for } z > z_c$$

with: $\alpha = \sqrt{Ri \frac{k^2+l^2}{k^2}} - \frac{1}{4}$ et $\epsilon = \pm 1$ such as $\epsilon \mathbf{k}U_0 > 0$.

This permits to evaluate

$$\overline{\mathcal{F}}(z) = -\frac{\rho_r 8\pi^2}{\pi L^2} \int_0^{+\infty} \frac{k^2 \Lambda^2}{V_0} \frac{\mathbf{k}}{\|\mathbf{k}\|} N |\hat{h}'|^2 (k, l = -k \frac{U(z)}{V_0}) dk$$



III Interaction between a front and an idealised mountain massive

Evaluation of inflow potential vorticity produced by \mathcal{F} and \mathcal{G} (Martin and Lott 2006)

The evolution for $q(x, y, z, t)$ is given by:

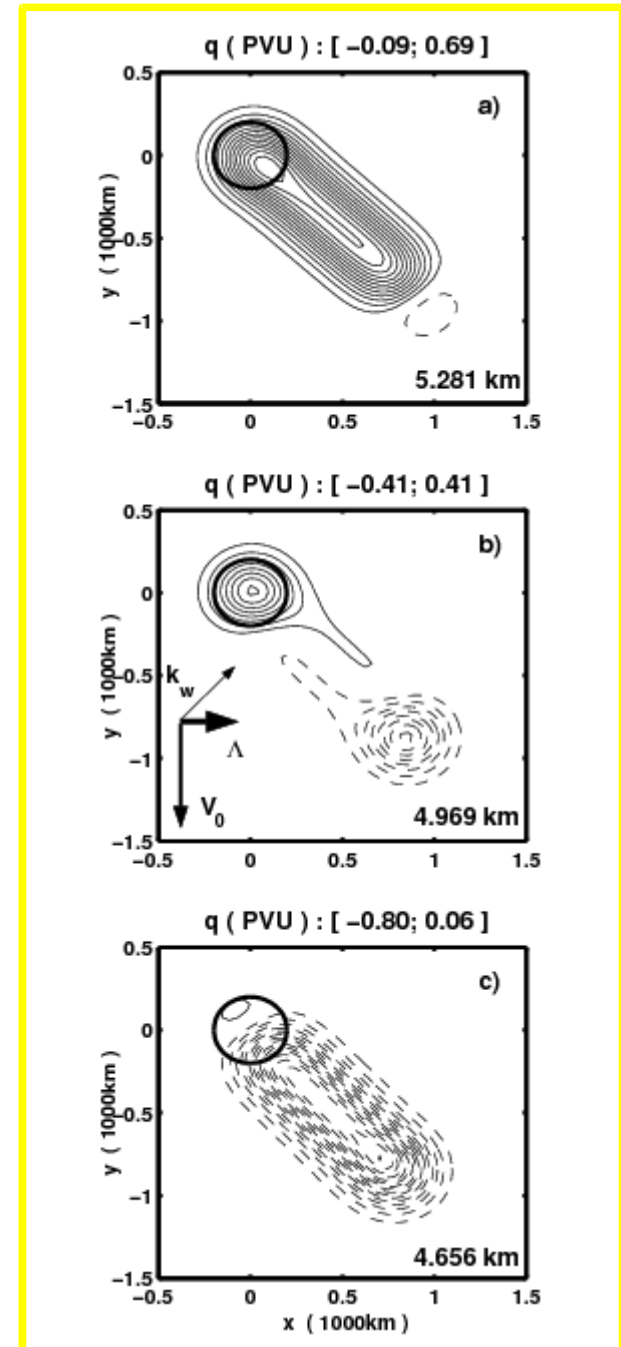
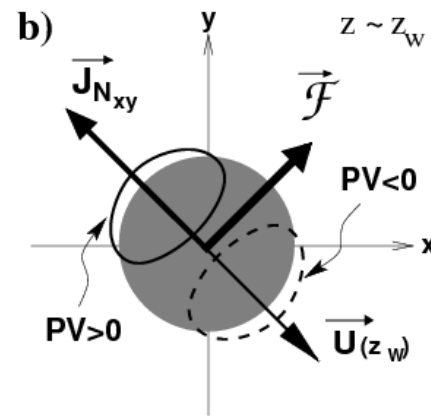
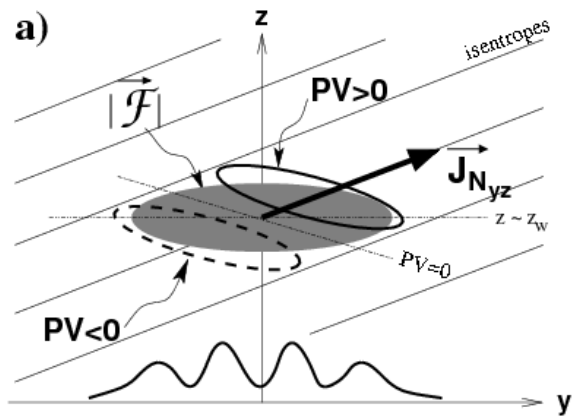
$$(\partial_t + \mathbf{U} \cdot \nabla) \rho_r q + \nabla \cdot \mathbf{J}_N = 0$$

where the non-advective flux

$$\mathbf{J}_N = -\theta_{0z} (1 - Ri^{-1}) \mathcal{G} \mathbf{e}_x + \theta_{0z} \mathcal{F} \mathbf{e}_y - \Theta_y \mathcal{F} \mathbf{e}_z$$

in the spectral space this yields to:

$$\rho_r \hat{q} = i \frac{1 - e^{i(\mathbf{k} \cdot \mathbf{U})t}}{\mathbf{k} \cdot \mathbf{U}} \left\{ \Theta_y \partial_z \hat{\mathcal{F}} + \theta_{0z} \left(-ik(1 - Ri^{-1}) \hat{\mathcal{G}} + i l \hat{\mathcal{F}} \right) \right\}$$



Note how the profile for q is quite different from that due to gravity waves breaking in a uniform background flow

III Interaction between a front and an idealised mountain massive

Influence at the ground of the potential vorticity produced by \mathcal{F} and \mathcal{G}

The potential vorticity and the geopotential are linked by the elliptic equation:

$$\frac{\partial^2 \hat{\phi}}{\partial z^2} - 2i\lambda_i \frac{\partial \hat{\phi}}{\partial z} - (\lambda_r^2 + \lambda_i^2) \hat{\phi} = \frac{g}{f\theta_r} \rho_r \hat{q}$$

A particular solution with no surface impact is first build:

$$\hat{\phi}_p(\mathbf{k}, z, t) = e^{-\lambda z} \int_0^z e^{2\lambda_r z'} \int_{z'}^D -\frac{g\rho_r}{f\theta_r} \hat{q} e^{-\lambda^* z''} dz'' dz'$$

The influence at the surface is then related to the boundary condition:

$$\lambda_r (\partial_t - i\mathbf{k} \cdot \mathbf{U}(\mathbf{0})) \hat{\phi}_u - ik\Lambda \hat{\phi}_u = (\partial_t - i\mathbf{k} \cdot \mathbf{U}(\mathbf{0})) \partial_z \hat{\phi}_p(0)$$

Eady Waves Dynamics Advection of the surface T anomaly associated with the PV anomaly q

Downstream effects:

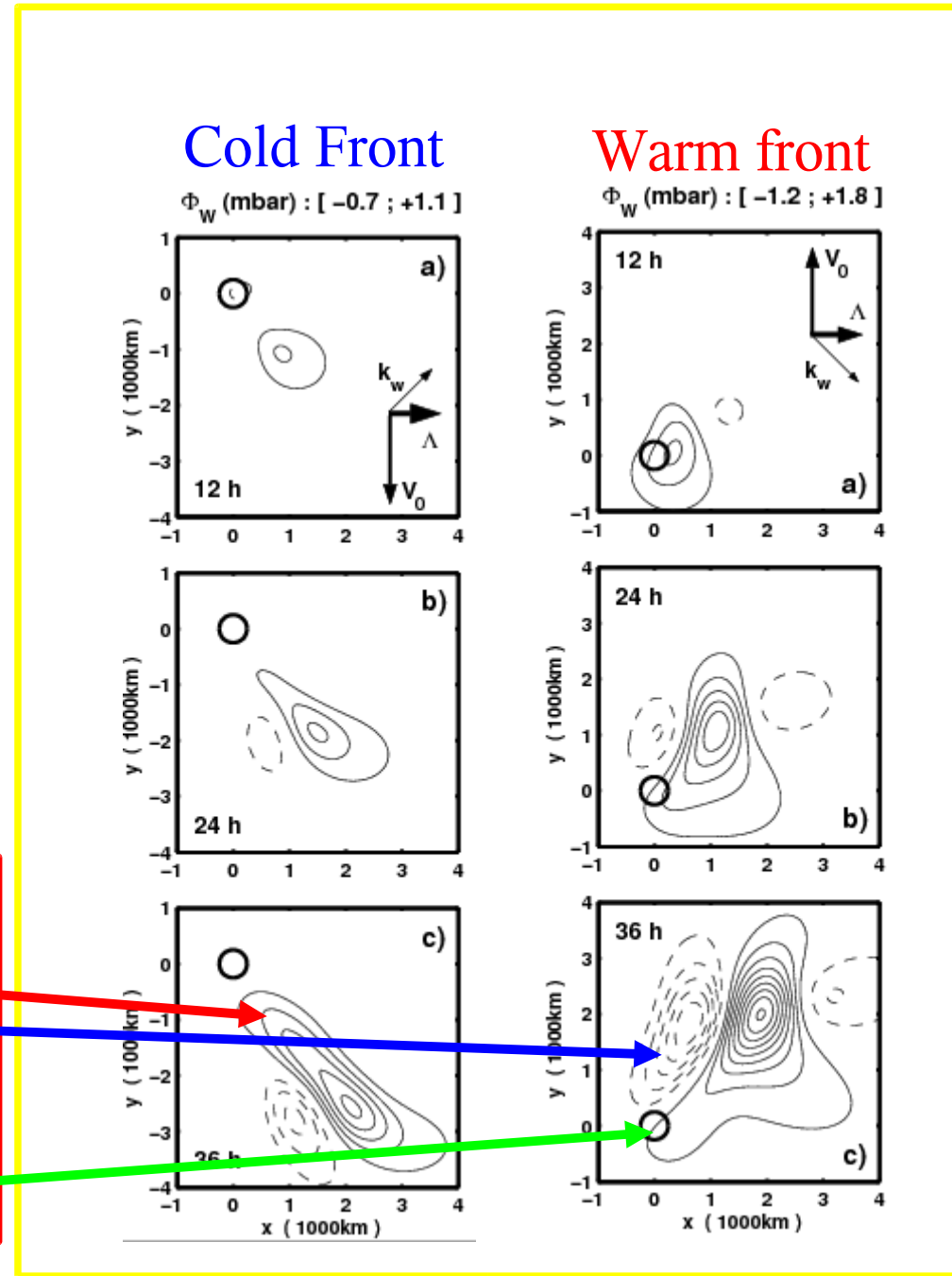
cyclonic for a cold front

cyclogénétique for a warm front

Effects over the mountain:

diminish the ridge for a cold front

increase the ridge for a warm front



III Interaction between a front and an idealised mountain massive

Influence at the ground of the potential vorticity produced by \mathcal{F} and \mathcal{G}

Downstream effects due to the Gravity Waves:

cyclolytic for a cold front (oppose to the effect of the envelope \mathcal{H})

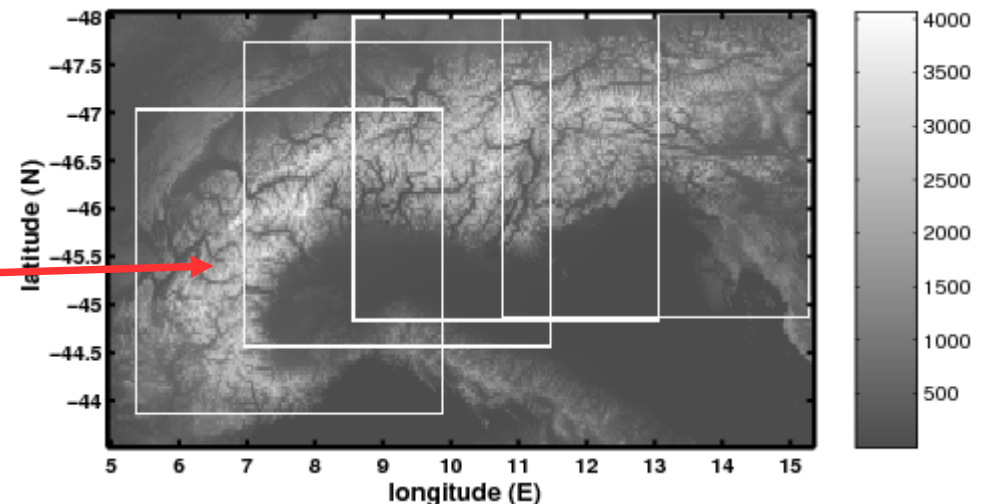
cyclogenetic for a warm front (reinforce the effect of the envelope \mathcal{H})

Effects over the mountain:

decrease the ridge for a cold front (oppose to the effect of the envelope \mathcal{H})

increase the ridge for a warm front (reinforce the effect of the envelope \mathcal{H})

**Those results stays valid
if we introduce a tropopause
(and baroclinic instabilities)
and if we take a more realistic
spectrum of the mountain**

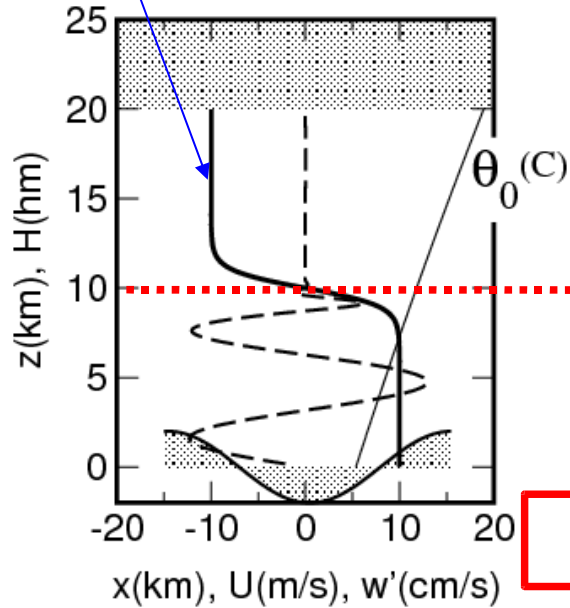


III Interaction between a front and an idealised mountain massive

Inertio Gravity Waves Re-emission (Lott 2003)

2D explicit simulations of Gravity Waves breaking with Coriolis Force

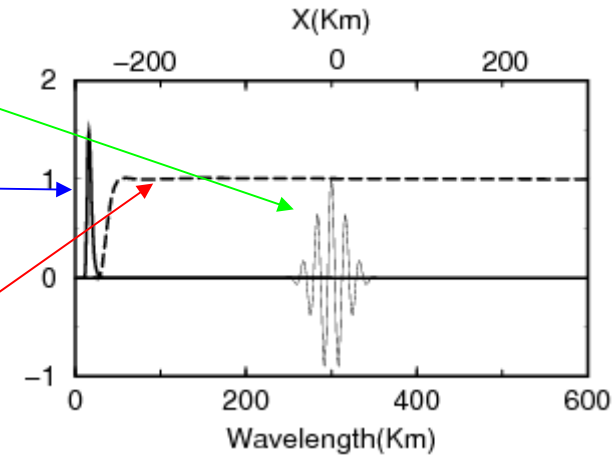
Incident wind U



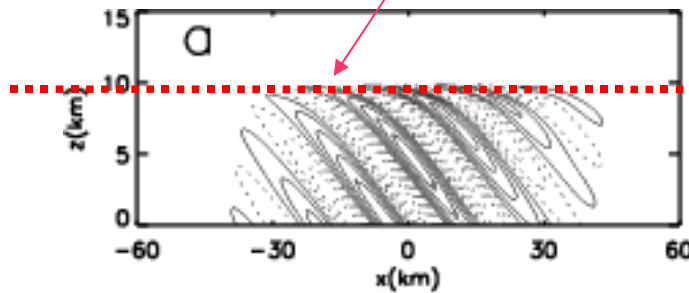
Mountain profile h'

h' spectrum'

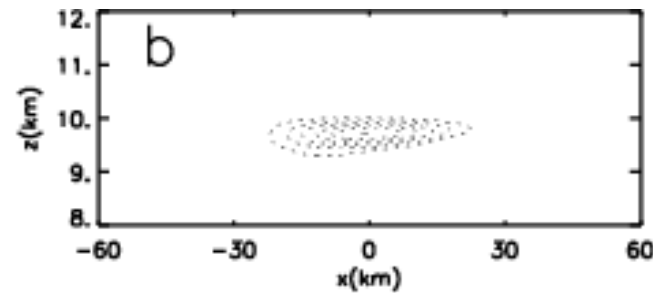
Low pass filter used to separate the large-scales and the small scales



Critical level



Vertical velocity associated with the Gravity Waves (non-filtered data)



Non-linear forcing due to the Gravity Waves breaking (Large-scale signal)

III Interaction between a front and an idealised mountain massive

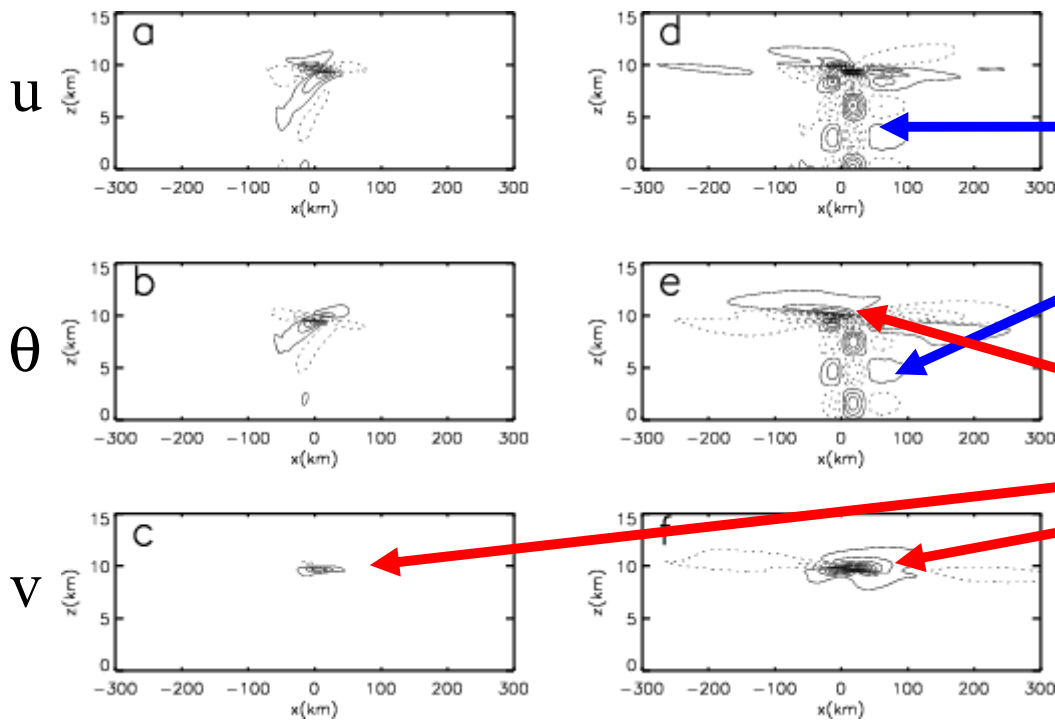
Inertio Gravity Waves Re-emission (Lott 2003)

2D explicit simulations of Gravity Waves breaking with Coriolis Force

Large-scale Response

t=6hrs

t=30hrs



Note:

The Inertio Gravity Waves that are re-emitted

The growing disturbance inside the shear layer (balanced part)

These 2 signals have a comparable amplitude

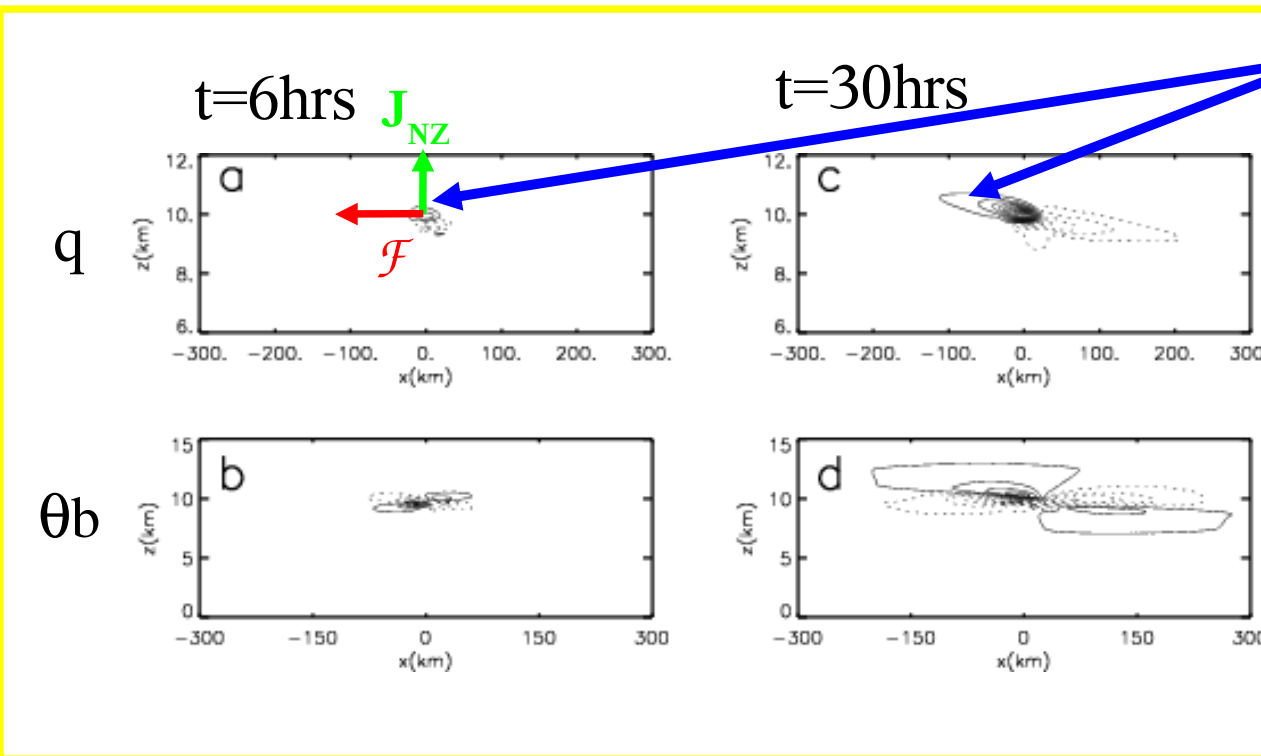
III Interaction between a front and an idealised mountain massive

Inertio Gravity Waves Re-emission (Lott 2003)

2D explicit simulations of Gravity Waves breaking with Coriolis Force

Note:

Large-Scale balanced response



The Potential vorticity anomaly (q) that grows with time:

q only results from the vertical component of the non-advective PV flux J_{NZ} (flux from below the Critical level to above)

q is then advected and steered by the mean flow

The Disturbance potential T is here estimated via the inversion of q

$$J_{NZ} = -\Theta_y \mathcal{F}$$

III Interaction between a front and an idealised mountain massive

Inertio Gravity Waves Re-emission

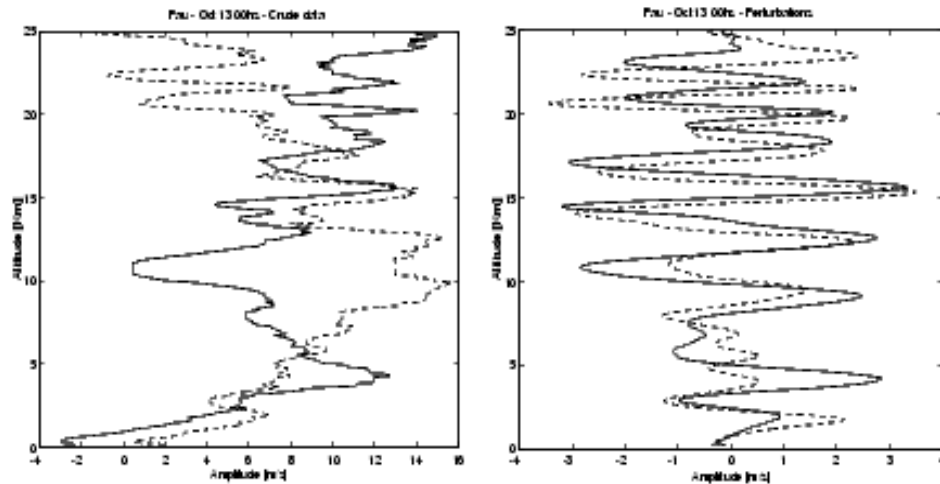
Observation after an intense mountain waves breaking event

(Scavuzzo Lamfri Teitelbaum and Lott 1998)

Observation: High resolution sounding launched from Pau the 13 October 1990
(u continuous, v dots)

Brut

Filtred



Polarization relationship between \hat{u} and \hat{v} :

$$\hat{v} = \frac{l\omega - ikf}{k\omega + ilf} \hat{u}$$

For waves resulting from a geostrophic adjustment:

$$\omega \approx f \text{ hence } \hat{v} \approx -i\hat{u}$$

PYREX Campain

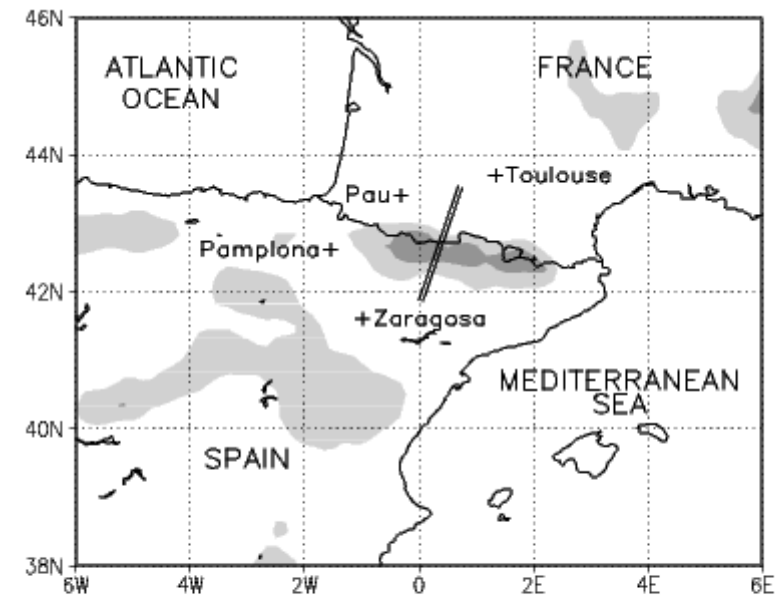


Figure 1: Smoothed terrain elevation and PYREX data used. + denotes the location of the high resolution soundings. The two thick lines indicate the airplane paths during the IOP 3. The light and dark shaded areas denote terrain elevation above 1000m and 1500m respectively.

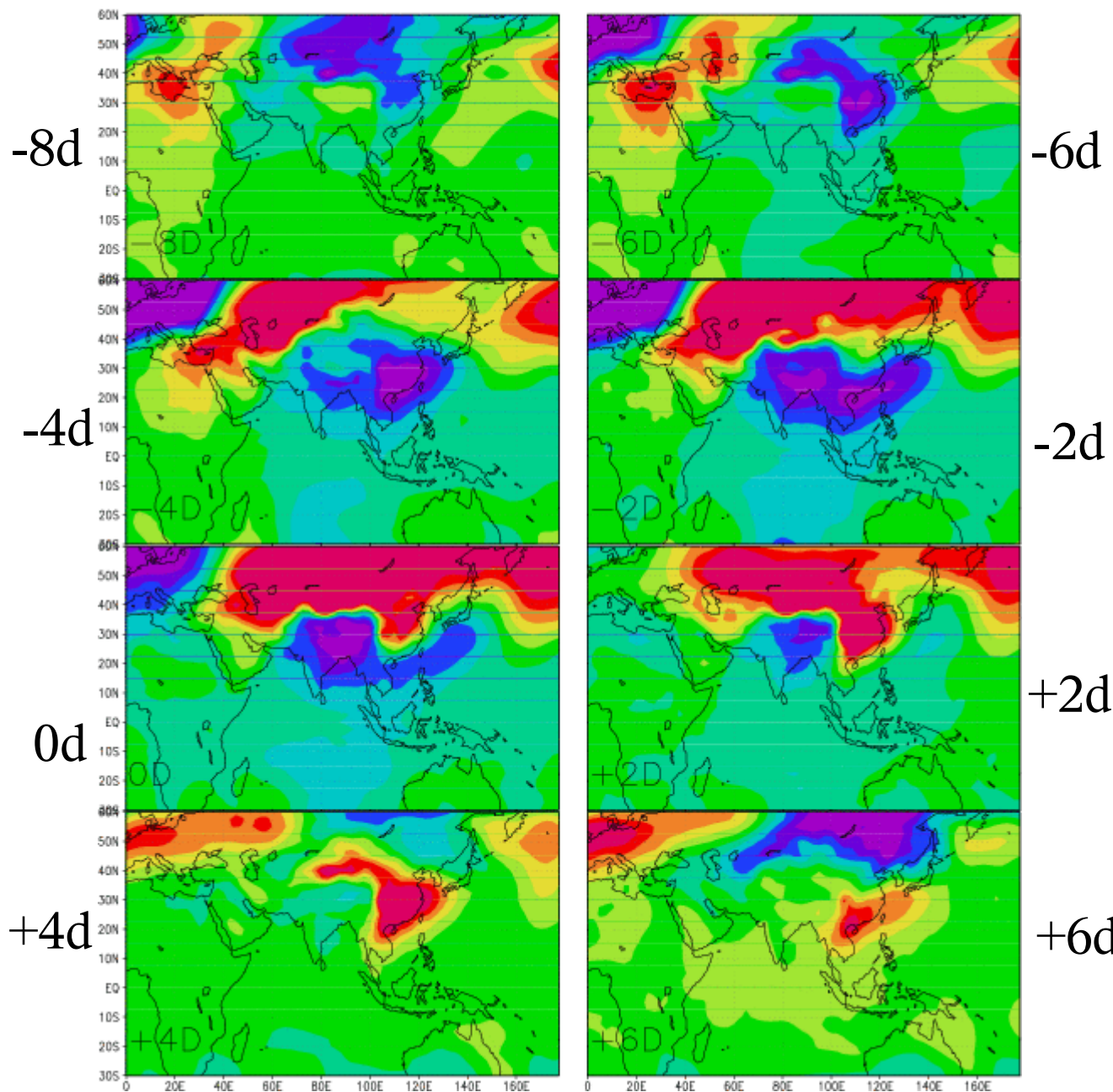
Summary

- Small-scale mountains have a significant impact on the climate
- In the middle atmosphere via the breaking of the mountain gravity waves (which affect the Brewer-Dobson circulation).
- In the low troposphere via nonlinear low-level flow dynamics, they affect the zonal mean zonal wind and the steady planetary wave.
- They have a potential influence on mountain lee cyclogenesis (this needs to be further analysed by mean of high resolution Limited Area Models)
- After their breaking, the mountain gravity waves can also re-emit inertio-gravity waves (to develop as well still by mean of high resolution Limited Area Models). Note that the Inertio Gravity Wave signal is a dominant one in the high resolution soundings travelling up to the low stratosphere.
- The parameterization of the directional critical levels has never been done. This would request to parameterize mountain gravity waves in the spectral space, as is done for non-orographic gravity waves.
- The interaction between mountain waves and the planetary boundary layer is still a poorly understood issue (Lott 2006).

III Interaction between a front and an idealised mountain massive

Variability over Eastern ASIA (NCEP data, Surface pressure)

ISL SLP COMPOSITE (70-03)
Key: Equatorial Himalayas Torqu



Composite of surface pressure keyed to the Himalaya Equatorial Pressure Torque
(an indicator of the dynamical influence of the massive on the Large-Scale flow):

Note the anomaly descending along the Eastern flank of the massive.

This is related to the so-called « Cold-Surges », strongly affecting the weather over Eastern Asia